Title
Indications of neutrino oscillations from an analysis of reactor experiments performed at different distances

Journal
Physical Review D, 27(1)

ISSN
2470-0010

Authors
Silverman, D
Soni, A

Publication Date
1983

DOI
10.1103/physrevd.27.58

PHYSICAL REVIEW D VOLUME 27, NUMBER 1 1 JANUARY 1983

Indications of neutrino oscillations from an analysis of reactor experiments performed at different distances

D. Silverman
Department of Physics, University of California, Irvine, California 92717

A. Soni
Department of Physics, University of California, Los Angeles, California 90024
(Received 4 January 1982)

A phenomenological analysis is presented of inverse-β (IB) experiments on proton targets performed at 6.5, 8.7, and 11.2 m from reactor sources and of a deuteron-disintegration experiment at 11.2 m. The analysis leads to the conclusion that either there is a statistically significant distance dependence of the $\bar{\nu}_e$ spectra measured in these experiments or that at least three of the four experiments have unstated sources of error or seriously understated errors. We find that this distance dependence can be accounted for by neutrino oscillations. The distance dependence is exhibited in the normalization-independent ratio of low- to high-energy halves of the spectrum. The ratios at the three distances, taken in pairs, differ by greater than 3 standard deviations. The entire analysis is done without using any theoretically calculated spectra. We find that no distance-independent spectrum can account for the 8.7- and 11.2-m IB experiments with a confidence level (C.L.) >0.026. Assuming neutrino oscillations rather than experimental errors are the cause of the distance dependence exhibited by the data we search for and find simple two-component neutrino-oscillation fits to the data with a gain in C.L. over the no-oscillation best fits by factors ranging from ~ 5 to ~ 15. These joint oscillation 2ν solutions have the $(\delta m^2, \sin^2 2\theta)$ values: $(0.95\pm 0.10\ \text{eV}^2, 0.32\pm 0.11)$, $(2.34\pm 0.23\ \text{eV}^2, 0.20\pm 0.07)$, and $(3.75\pm 0.27\ \text{eV}^2, 0.25\pm 0.08)$. Under the 3ν hypothesis the solutions have the values $\delta m^2_{12}=0.88^{+0.16}_{-0.24}\ \text{eV}^2$ and $\delta m^2_{13}=2.39\pm 0.30\ \text{eV}^2$, with amplitudes $0.17^{+0.13}_{-0.08}$ and 0.16 ± 0.08, respectively. The limits quoted correspond to 90% C.L. obtained by including the reactor $\bar{\nu}_e$ spectral range from inversion of the e^- spectrum from the fission of ^{235}U and by disregarding the 6.5-m experiment on the grounds that it has poor statistics for analysis of its differential spectrum. Each one of these solutions is within the 68%-C.L. allowed region in the $(\delta m^2, \sin^2 2\theta)$ space of the analysis by Boehm *et al.* of their own experiment at 8.7 m. The above oscillation parameters are within the allowed limits from accelerator experiments. Our observation of the difference between the 8.7- and 11.2-m IB experiments on proton targets may constitute new evidence for $\bar{\nu}_e$ oscillations, provided the experiments are correct.

I. INTRODUCTION

In this paper we report a phenomenological analysis[1,2] for neutrino oscillations of the data from reactor experiments performed at different distances.

There are four experiments that are being used in our analysis. Three of these involve the inverse-β (IB) reaction

$$\bar{\nu}_e + p \rightarrow n + e^+ \tag{1.1}$$

experimentally studied at 6.5 (Ref. 3), 8.7 (Ref. 4), and 11.2 m (Ref. 5) from reactor sources. The 6.5-m experiment is the earliest experiment and had only about 500 events whereas the 8.7-m and 11.2-m experiments, data from which became available only recently, had about 5000 and 7000 events, respectively.

In addition to these three IB experiments we include the deuteron experiment[6] of Reines, Sobel, and Pasierb (RSP) in our analysis. This experiment involved a measurement of the disintegration of the deuteron at 11.2 m from a reactor source (with about 6000 events) via the neutral- and charged-current reactions

$$\bar{\nu} + d \rightarrow n + p + \bar{\nu}\,, \tag{1.2}$$

$$\bar{\nu}_e + d \rightarrow n + n + e^+\,, \tag{1.3}$$

resulting in one-neutron and two-neutron events, respectively. We recall that RSP cited the difference between the measured value of the ratio [rate for reaction (1.3)]/[rate for reaction (1.2)] compared to its expected value based on calculated reactor $\bar{\nu}_e$ spectra as evidence for neutrino instability.

We also include in our analysis the measurement[7,8] of the e^- spectrum from fission of U^{235} and the range of $\bar{\nu}_e$ spectra consistent with it.

The main objectives of this study are (1) to introduce a framework for analysis of reactor experiments independent of theoretically calculated reactor $\bar{\nu}_e$ spectra, (2) to find sensitive tests for searching for oscillations in such experiments, (3) to determine if the present data show a statistically significant distance dependence of the $\bar{\nu}_e$ spectrum, (4) to find if this is consistent with neutrino oscillations and to solve for the most favorable oscillation parameters, and (5) to suggest the most favorable distances for detecting $\bar{\nu}_e$ oscillations in such experiments. So far as the overall conclusions reached about the existence or nonexistence of $\bar{\nu}_e$ oscillations are concerned they will necessarily be dependent on the accuracy of the input experimental data.

In the interplay of the experiments mentioned above we find that the energy spectra of $\bar{\nu}_e$ measured at different distances are not compatible. The main source of distance dependence exhibited by the data is a systematic depletion of $\bar{\nu}_e$ (of energy $\gtrsim 6$ MeV) with increase in distance from 6.5 to 11.2 m. In particular there are two completely independent experiments monitoring $\bar{\nu}_e$ at 11.2 m, namely, the IB reaction (1.1) and the charged-current deuteron reaction (1.2) and *both* of these experiments report seeing fewer high-energy ($E_\nu \gtrsim 6$ MeV) $\bar{\nu}_e$ at 11.2 m than seen at 8.7 m and far fewer than were seen at 6.5 m.

We quantitatively assess this distance dependence in three interrelated ways:

(i) From an IB experiment performed at a given distance we deduce the corresponding neutrino spectrum and compute the ratio for two bins,

$$R_\nu = 1 + \frac{\text{No. of } \bar{\nu}_e \text{ "seen" with } (4.0 < E_\nu < 6.7 \text{ MeV})}{\text{No. of } \bar{\nu}_e \text{ "seen" with } (6.7 < E_\nu < 8.5 \text{ MeV})} . \tag{1.4}$$

We find that $R_\nu = 6.6 \pm 1.8$, 13.6 ± 1.2, and 21.7 ± 2.6 at 6.5, 8.7, and 11.2 m. Taken in pairs these numbers differ by $\gtrsim 3$ standard deviations.

(ii) From the 11.2-m IB and the deuteron experiments the ratio

$$r_d = \frac{\text{rate of charged-current deuteron events/day}}{\text{rate of neutral-current deuteron events/day}} \tag{1.5}$$

is found to be 0.23 ± 0.06. The measured $\bar{\nu}_e$ energy spectra at 8.7 and 6.5 m allow one to calculate the value of r_d implied by each of those spectra. If neutrinos do not oscillate then the values of r_d implied by the 6.5 and 8.7m IB experiments should agree with the measured value of r at 11.2 m. We find that they disagree by $\gtrsim 2.5$ standard deviations (SD).

(iii) By assuming that the reactor $\bar{\nu}_e$ spectrum is expressible in the form $\exp[\sum_{j=0}^{N} A_j (E_\nu/\text{MeV})^j]$ with arbitrary A_j's and N (the justification for assuming that the spectrum is a smooth function of neutrino energy is given later) we show that no such no-oscillation spectrum can account for the data from all the four reactor experiments performed at different distances with a confidence level (C.L.) > 0.0036. Indeed the maximum confidence level attainable for a no-oscillation spectrum to account for the overlapping data from the 8.7- and 11.2-m high-statistics IB experiments alone is found to be C.L. $= 0.026$.

Assuming that neutrino oscillations, rather than experimental inaccuracies, are the cause of the distance dependence mentioned above, we search for joint oscillation solutions to all the reactor experiments. Three solutions with oscillations among 2ν species fit the joint reactor data. These have the following parameters (ranges quoted correspond to 90% C.L.):

(a) $\delta m^2 = 0.95 \pm 0.10 \text{eV}^2$,
$\sin^2 2\theta = 0.32 \pm 0.11$,

(b) $\delta m^2 = 2.34 \pm 0.23 \text{eV}^2$,
$\sin^2 2\theta = 0.20 \pm 0.07$,

(c) $\delta m^2 = 3.75 \pm 0.27 \text{eV}^2$,
$\sin^2 2\theta = 0.25 \pm 0.08$.

Under the 3ν hypothesis the solutions have the values $\delta m^2_{12} = 0.88^{+0.16}_{-0.24}$ eV^2 and $\delta m^2_{13} = 2.39 \pm 0.30$ eV^2 with amplitudes $0.17^{+0.13}_{-0.08}$ and 0.16 ± 0.08, respectively.

In conjunction with each of these oscillation solutions we solve for the reactor $\bar{\nu}_e$ spectrum that fits the data. The resulting spectra are found to be compatible with the range of the reactor $\bar{\nu}_e$ spectra obtained from the inversion of the β spectrum from fission of ^{235}U measured by Carter, Reines, Wagner, and Wyman[7] (1959) and by Schreckenback *et al.* (1981).[8]

The set of oscillation parameters that emerge from this analysis is compared with the values allowed for these parameters by existing accelerator experiments.[9–13] Existing limits on $\nu_e \rightarrow \nu_\tau$ do not exclude any of our solutions. For the $\nu_\mu \rightarrow \nu_e$ limits the $\delta m^2 \simeq 0.9$ eV^2 solution is not excluded but the $\delta m^2 \simeq 2.3$ eV^2 and $\delta m^2 \simeq 3.7$ eV^2 solutions appear excluded at the 90% C.L. from being mainly $\bar{\nu}_e \rightarrow \bar{\nu}_\mu$.

In particular, we stress that our three solutions are within the 68%-C.L. allowed region in δm^2 vs $\sin^2 2\theta$ space of the analysis by Boehm *et al.* of their own experiment at 8.7 m.[4]

We find that our oscillation solutions favor smaller mixing angles (of the order of the Cabibbo angle) compared to the solution obtained by RSP,[6] but we are compatible with their analysis at the 90% C.L.

In this paper there are several additions to the analysis reported in our Physical Review Letter.[1] These are (1) an analysis using the weighted mean of the charged-current deuteron reaction measured directly at 11.2 m and calculated from the measured 11.2-m spectra, (2) the inclusion of energy-calibration uncertainties and effects of the relaxation of their constraints, (3) the determination of the range of $\bar{\nu}_e$ spectra and using this as another experimental constraint on the fits, (4) the calculation of C.L. contours in the $\sin^2 2\theta$, δm^2 plane, and (5) a demonstration of the consistency of our analysis with the accelerator experiments.

In Sec. II the IB reaction on protons and its detection are discussed. In Sec. III we present our method of fitting to the reactor spectra and the justification of the effective identity of the Savannah River Plant (SRP) and Institut Laue-Langevin (ILL) reactor spectra. In Sec. IV the experimental input data are discussed. In Sec. V the $\bar{\nu}_e$ spectra are determined at each experimental distance and their shape differences demonstrated. In Sec. VI the consistency of the charged-current deuteron measurement at 11.2 m with the IB spectra at 11.2 m is shown. In Sec. VII the distance dependence is demonstrated in three different ways and shown to remain even after relaxation of experimental uncertainties. In Sec. VIII we discuss the inversion of the measured e^- β-decay spectrum from ^{235}U fission into a range of associated $\bar{\nu}_e$ spectra depending on the nuclear Z value. In Sec. IX is presented the neutrino-oscillation formalism for many neutrinos and the pseudo-2ν cases arising from possible large-mass ratios. In Sec. X are presented the most likely 2ν oscillation fits and the contours in the δm^2, $\sin^2 2\theta$ plane as well as the gain in C.L. over the best no-oscillation fit. In Sec. XI is presented the analysis of the 3ν cases that appear as pseudo-2ν oscillations. Section XII presents the maximum-likelihood 3ν oscillation fit and contours. In Sec. XIII the lower-statistics 6.5-m experiment is included in the joint analysis. In Sec. XIV the oscillation solutions to the reactor data are shown to be consistent with bounds from accelerator experiments. Section XV discusses the sensitivity of new reactor experiments to the oscillation solutions and Sec. XVI presents our conclusions and summary.

II. INVERSE-β REACTION

The e^+ energy spectrum has been experimentally measured at 6.5 (Ref. 3), 8.7 (Ref. 4), and 11.2 m (Ref. 5) from reactor $\bar{\nu}_e$ sources via the inverse-β reaction:

$$\bar{\nu}_e + p \rightarrow n + e^+ . \tag{2.1}$$

Since the relevant reactor $\bar{\nu}_e$ energies are $\lesssim 10$ MeV, the nonrelativistic positron kinetic energy is given by

$$E_e' = E_\nu - (m_n - m_p + m_e) = E_\nu - 1.80 \text{ MeV} \tag{2.2}$$

and the cross section for (2.1) is given by

$$\sigma(E_\nu) = 9.24 \times 10^{-44} (E_\nu - 1.29) \times [(E_\nu - 1.29)^2 - 0.26]^{1/2} \text{ cm}^2 , \tag{2.3}$$

where E_ν is the incident neutrino energy in MeV. The differential rate for e^+ with observed kinetic energy E_e at a distance L from a reactor source is given by

$$\frac{dR}{dE_e}(\text{No. /MeV day}) = 0.203 \times (9.24 \times 10^{-44} \text{cm}^2)^{-1} \left[\frac{P}{1 \text{ MW}}\right] \left[\frac{n_p}{10^{26}}\right] \left[\frac{L}{1 \text{ m}}\right]^{-2} \eta_s \times \int dE_e' \, \sigma(E_\nu) R_e(E_e, E_e') \eta(E_e') n(E_\nu, L) , \tag{2.4}$$

where P is the reactor power, n_p is the number of protons in the target, $R_e(E_e,E_e')$ is the experimental energy-resolution function

$$R_e(E_e,E_e')=\frac{1}{\sqrt{2\pi}\tilde{\sigma}(E_e')}\exp\left[-\frac{(E_e-E_e')^2}{2\tilde{\sigma}(E_e')^2}\right], \tag{2.5}$$

$\eta(E_e')$ is the energy-dependent detection efficiency, η_s the energy-independent systematic efficiency, $n(E_\nu,L)$ is the spectrum (No. of $\bar{\nu}_e$/fission MeV) of $\bar{\nu}_e$ with energy E_ν at distance L from the reactor source, and $\tilde{\sigma}(E_e')$ is the energy resolution.

III. REACTOR $\bar{\nu}_e$ SPECTRA

A. Method of fitting

In our analysis we shall not use any of the theoretically calculated spectra[14–19] which deviate from each other as much as $\pm 30\%$. Instead we solve for the reactor $\bar{\nu}_e$ spectra which are compatible with the experimental data separately under the oscillation and the no-oscillation hypotheses. For that purpose we assume that the reactor ν_e spectrum $n_0(E_\nu)$ can be parametrized in the general form

$$\ln[n_0(E_\nu)]=\sum_{j=0}^{N} A_j(E_\nu/1\ \text{MeV})^j . \tag{3.1}$$

χ^2 minimization is then used to deduce A_j and N from the observed e^+ spectra. To elaborate, suppose we want the best no-oscillation fit to the $\bar{\nu}_e$ spectrum. We take

$$n(E_\nu,L)=n_0(E_\nu)=\exp\left[\sum_{j=0}^{N} A_j E_\nu{}^j\right]$$

as in (3.1) and substitute its explicit form in (2.4) starting with a given N. Then Eq. (2.4) is used to calculate the e^+ rates $(dR/dE)_{\text{theor}}$ for e^+ energies corresponding to all the experimental data points under consideration. We then calculate the sum total of the χ^2, $\chi^2(N)$:

$$\chi^2(N)=\sum_i\left[\frac{(dR/dE_i)_{\text{theor}}-(dR/dE_i)_{\text{expt}}}{(\sigma_i)_{\text{expt}}}\right]^2, \tag{3.2}$$

where the sum runs over all the data points. The coefficients A_j that characterize the spectrum are then solved for numerically by minimizing $\chi^2(N)$.

We may start at $N=2$, for example, and then repeat the procedure for $N=3,4,5\ldots$, etc., and the corresponding 3,4, or 5... coefficients A_j are solved for. For each value of N there is a corresponding minimum value of $\chi^2_{\min}(N)$. If one plots of $\chi^2_{\min}(N)/d_f(N)$, where $d_f(N)$ is the number of degrees of freedom (i.e., number of data points minus number of parameters used) versus N one finds a curve that shows a fast drop with increase in N, reaches a "global minimun," and starts increasing very slowly. The slow increase results from a decrease in $d_f(N)$ as N increases.

When we test the experimental data taken at different distances against the oscillation hypothesis we will take

$$n(E_\nu,L)=\exp\left[\sum_{j=0}^{N} A_j(E_\nu/1\ \text{MeV})^j\right]\times P_{\bar{\nu}_e}(E_\nu,L) , \tag{3.3}$$

where $P_{\bar{\nu}_e}(E_\nu,L)$ is the probability of survival of $\bar{\nu}_e$ of energy E_ν at distance L from the reactor source. Then using the same χ^2 minimization procedure we solve for A_j's, N, and the oscillation parameters simultaneously.

It should be clear that the theoretically calculated spectra, e.g., of Ref. 14 or 15, can be cast in the form of (3.1) with a very specific set of coefficients. Therefore when we test the data for the no-oscillation hypothesis by allowing A_j and N to be totally arbitrary we are indeed being very conservative; that is, if the experimental data cannot be accounted for with any A_j's and N then it certainly cannot be accounted for by any calculated spectra. In other words, for the no-oscillation case, the C.L. for the fits to the data based on the theoretically calculated spectra would be far worse than for our general fit with A_j and N arbitrary.

We give here a justification for the assumption that the reactor $\bar{\nu}_e$ spectrum is a smooth function of neutrino energy. As is well known all the $\bar{\nu}_e$ originate from β decays with a continuous distribution of neutrino energy and hundreds of decays contribute. We thus expect the reactor $\bar{\nu}_e$ spectrum to be a smooth function of neutrino energy. Indeed all the present evidence suggest that the reactor $\bar{\nu}_e$ spectrum is a relatively smooth function of neutrino energy and can in fact be sufficiently well fitted by the general form of Eq. (3.1). These evidences are (1) the measured β spectrum from fission of ^{235}U (see Sec. VIII), (2) the central values of the $\bar{\nu}_e$ spectrum resulting from the inversion of that measured β spectrum (see Sec. VIII), (3) all

theoretically calculated reactor $\bar{\nu}_e$ spectra of Refs. 14–19, and (4) the reactor $\bar{\nu}_e$ spectrum monitored at each distance. All are expressible in the form of Eq. (3.1).

B. Spectra of SRP and ILL reactors

The 57-MW research reactor at Institut Laue-Langevin (ILL) used in the 8.7-m experiment produces essentially only the ^{235}U fission spectrum. The ~2000-MW isotope production reactor at Savannah River Plant (SRP) used in the 6.5- and 11.2-m experiments is cycled about every six weeks and therefore maintains a fairly constant and low level of other fissionable nuclei. The average percentage of fissions at SRP by nuclide is ^{235}U 88%, ^{239}Pu 8%, ^{238}U 4%. We can use the calculated fission spectra of these isotopes good to 10–20% to get a highly accurate calculation of the *differences* of the SRP and ILL spectra from the 12% isotope difference. The ^{239}Pu spectra is softer and the ^{238}U is harder than ^{235}U leading to cancellations. The calculated spectral difference is at most 1.5% from $E_\nu=2$ to 8 MeV and differs in shape by only 1% from $E_\nu=2$ to 7.5 MeV. The error range expected assigning 20% errors to the spectra of Ref. 16 (which differ by up to 16% from their previous spectra Ref. 15) for a 12% change in fission nuclides bounds the actual differences at ±2.4%. Thus no account of the 1% shape difference was used in our calculations. The ^{235}U and ^{239}Pu fissions are triggered by thermal neutrons and the temperature differences in the reactors can have no effect on the MeV scale of nuclear fissions. The fissioning percentages of the SRP reactor during the 1963–1965 period of the 6.5-m experiment had the average values of ^{235}U 82.8%, ^{239}Pu 9.5%, and ^{238}U 7.7%. Using the calculations of Ref. 16 for the differences this yields a spectrum that differs from that of ^{235}U by less than 1% for $1 < E_\nu < 7$ MeV.

IV. CHARACTERISTICS OF THE INPUT EXPERIMENTAL DATA

We now describe the characteristics of the experimental data that are relevant to our work. For the 11.2-m experiment we used nine data points in the positron energy interval $2.2 \leq E_e \leq 6.7$ MeV. Most of the data points have statistical errors of about 4 to 20% whereas the overall normalization uncertainty is 14%. We used 19 data points from the 8.7-m experiment with $1 \lesssim E_e \lesssim 6.7$ MeV. These have larger statistical errors (10 to 30% in general) but the estimated normalization error is only 8%.

For the 6.5-m experiment it is important to note that in the e^+ spectrum given (Fig. 11 of Ref. 3) as well as in the formula for the required $\bar{\nu}_e$ spectrum [given in Eq. (16) of Ref. 3] the reactor-off background was not subtracted. It was, of course, subtracted in their final expression for the total cross section. There are 16 points with $1 \leq E_e \leq 8$ MeV in this experiment. These have fairly large statistical errors (calculated from their Table VI, using Poisson statistics) ranging from about 25 to 100% because the reactor-off background was obtained for only $\frac{1}{7}$ of the reactor-on time. We emphasize that while for the main purpose of that experiment, that is, a measurement of the total cross section, the background determination was accurate enough, it is poorly determined so far as the detailed shape of the e^+ spectrum is concerned. Therefore implications deduced by use of the detailed shape of the e^+ spectrum from that experiment alone may be quite misleading.

The deuteron experiment of RSP[6] was also performed at 11.2 m from the reactor source and provides a measurement of the rates [(165±25)/day] for the neutral-current deuteron (ncd) reaction

$$\bar{\nu}+d \rightarrow n+p+\bar{\nu} \tag{4.1}$$

and [(238±12)/day] for the charged-current deuteron (ccd) reaction

$$\bar{\nu}_e+d \rightarrow n+n+e^+ . \tag{4.2}$$

In the theoretical calculation for the deuteron rates we used the parameters[20,21] (in usual notation) $a_s^{np}=0.12$ MeV, $r_s^{np}=0.0139$ MeV^{-1}, $a_s^{nn}=0.094$ MeV, and $r_s^{nn}=0.0142$ MeV^{-1}. We emphasize that the effective-range correction incorporated in our analysis reduces both the rates by 5 to 8%.

The energy-resolution functions of the three IB experiments are of the form (2.5) and have resolution Gaussian widths:

$$\begin{aligned} &6.5\ m:\ \tilde{\sigma}=0.106\ \text{MeV}\sqrt{E_e}\ , \\ &8.7\ m:\ \tilde{\sigma}=0.073\ \text{MeV}\sqrt{E_e}\ , \\ &11.2\ m:\ \tilde{\sigma}=0.194\ \text{MeV}\sqrt{E_{\text{obs}}}\ , \end{aligned} \tag{4.3}$$

where $E_{\text{obs}}=E_e+0.32$ MeV, and E_e is in MeV.

V. INDIVIDUAL $\bar{\nu}_e$ SPECTRA

The $\bar{\nu}_e$ spectrum monitored at each distance can be obtained by substituting the parametrization

(3.1) into Eq. (2.4). We use the measured e^+ energy spectrum and numerically solve for the coefficients A_j and the degree N such that the χ^2 is minimum using only the statistical errors of the experimental data. Thus the solutions for $A_0, A_1, \ldots, A_5$ for each experiment are

$$\begin{aligned}
&6.5\text{ m: } 3.837, -1.6401, 0.071\,93, 0, 0, 0,\ \chi^2/d_f = 0.44/2\ ;\\
&8.7\text{ m: } 1.558, -0.5102, -0.055\,83, 0, 0, 0,\ \chi^2/d_f = 15.4/16\ ;\\
&11.2\text{ m: } 0, 0.8298, -0.520\,15, 0.079\,335, -0.005\,323, 0,\ \chi^2/d_f = 6.2/5\ .
\end{aligned} \tag{5.1}$$

Each of these has an energy-independent overall uncertainty; these are 10%, 8%, and 14%, respectively. These spectra (times the IB cross section) versus E_e (on a logarithmic scale), shown in Fig. 1, exhibit an interesting trend. For $2 \leq E_e \leq 4.5$ MeV the 6.5-m spectrum is the lowest and the 11.2-m one is the highest with the 8.7 m lying between the two. For $E_e \gtrsim 4.5$ MeV that ordering is reversed. Irrespective of the overall normalization or multiplicative changes in energy calibration shifts, the spectra have remarkably different shapes or concavity. The band and bars shown on Fig. 1 indicate the 1-SD ranges obtained by using the covariance matrix. While the values of the $\bar{\nu}_e$ spectrum deduced for a given value of $\bar{\nu}_e$ energy differ from one experiment to another by (at most) a few standard deviations it is important to recognize the trend: Each data point in the 11.2-m experiment for $E_e \gtrsim 4.5$ MeV lies below the 8.7-m experiment. This is also seen if one goes back to use the measured e^+ histograms for $E_e \gtrsim 4.5$ MeV. Later we shall exhibit an optimal statistical analysis of these trends. The plot of Fig. 1 contains the magnitude logarithmically so that a shift in normalization of any spectra only moves it vertically without altering the shape or curvature. Similarly the energy is plotted as the $\ln E_e$ so that multiplicative calibration shifts $E_e^{\text{true}} = (1+\epsilon)E_e^{\text{meas}}$ will only shift the spectra horizontally without a shape change. Clearly the curves cannot be made to agree with only normalization or calibration shifts.

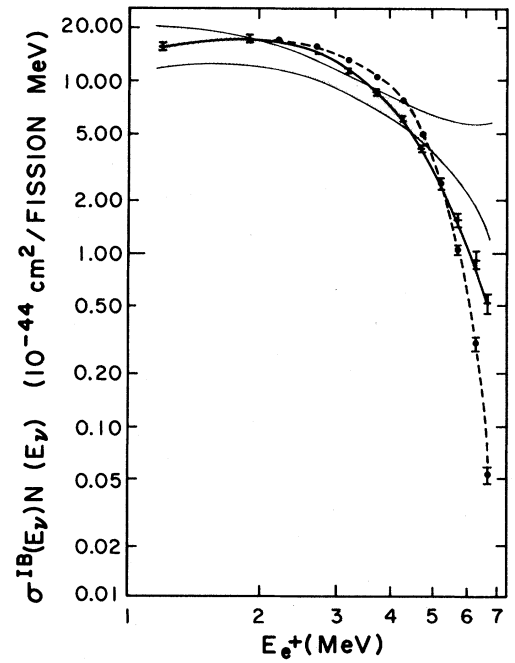

FIG. 1. $\sigma(E_\nu)N_\nu(E_\nu)$ vs E_e (in a double logarithmic plot) for fits to the IB experiments at each distance separately. The wide error band is for the 6.5-m data, the solid curve is for the 8.7-m data, the dot-dashed curve for the 11.2-m data. Multiplicative changes in normalization or energy calibration only shift the curves vertically or horizontally, respectively, but cannot alter their shapes.

VI. CONSISTENCY OF THE IB AND THE ccd MEASUREMENT AT 11.2 m

There are two independent experiments initiated by $\bar{\nu}_e$ at 11.2 m, namely, the IB experiment [reaction (1.1)] and the deuteron experiment [reactions (1.2) and (1.3)]. The latter experiment measures the rates for the disintegration of the deuteron via the charged weak current and via the neutral weak current. The neutral-current reaction on the deuteron is not sensitive to the type of neutrino initiating the reaction.[22] However, the charged-current deuteron reaction is triggered only by $\bar{\nu}_e$.

Thus the IB experiment (on a proton target) and the ccd experiment (on a deuterium target) are two independent experiments monitoring $\bar{\nu}_e$ at 11.2 m. While the IB experiment measured the shape of the $\bar{\nu}_e$ energy spectrum the ccd experiment measured only the total rate (via counting the $2n$ events) and found it to be (28 ± 12) events/day. The measured $\bar{\nu}_e$ spectrum via the IB experiment at 11.2 m allows one to calculate the expected number of $2n$ events to be

$$\begin{aligned}
&= 45.03 \pm 0.53(\text{statistical})\\
&\quad \pm 6.2(\text{normalization})\\
&\quad \pm 8.3(e^+\text{energy calibration})\\
&= 45.0 \pm 10.4\ .
\end{aligned} \tag{6.1}$$

The last error is due to the 2.5% uncertainty in the e^+ energy calibration of the IB experiment. The observed spectrum is falling steeply with energy for $E_\nu \gtrsim 6$ MeV where most of the ccd reaction arises from. The calibration uncertainty is, therefore, a major source of error and is important for a correct understanding of the interplay of the IB experiment and the charged-current deuteron experiment. This source of error has not been taken into account in previous works on this subject.

The ccd measured rate of (28 ± 12) events per day differs from that implied by the IB experiment of (45.0 ± 10.4) by 1.07 SD. This difference of approximately 1 SD is between two entirely different experiments determining the ccd rate. We therefore take the weighted mean of the two numbers and conclude that the rate for the ccd reaction at 11.2 m is given by

$$\bar{\Gamma}(\text{ccd})_{11.2}=(37.3\pm8.0)\text{events /day} . \quad (6.2)$$

Each ccd rate now differs from the weighted mean by less than 1 SD. The deuteron experiment measured the ncd rate to be (165 ± 25)/day. Thus at 11.2 m we have

$$\bar{r}_{11.2}=\frac{\bar{\Gamma}(\text{ccd})}{\Gamma(\text{ncd})}=\frac{37.3\pm8.0}{165\pm25}=0.23\pm0.06 . \quad (6.3)$$

From the ccd measured rate of (28 ± 12)/day and the one implied by the IB experiment of (45 ± 10)/day it is clear that the "true" spectrum of $\bar{\nu}_e$ at 11.2 m is even softer than that represented by the fit (5.1) to the 11.2-m IB experiment alone. We, therefore, now calculate a fit to the $\bar{\nu}_e$ spectrum monitored at 11.2 m using nine data points from the e^+ histogram measured via the IB reaction and the total ccd rate of (28 ± 12)/day as an additional data point. The resulting joint fit for $\bar{\nu}_e$ at 11.2 m $(A_0,A_1,\ldots,A_5)$ is

$$\overline{11.2\text{ m}}:\ 0,0.826,-0.5208,0.079\,22,$$
$$-0.005\,345,0,\ \chi^2/d_f=7.6/6 . \quad (6.4)$$

This spectrum is somewhat softer than the fit [Eq. (5.1)] to the 11.2-m IB experiment alone and it gives a ccd rate of 40.8/day.

We note that the ccd and ncd rates above can be converted into reactor-weighted cross sections in units of 10^{-44} cm^2/fission by dividing the rates by 57.5 events/day.

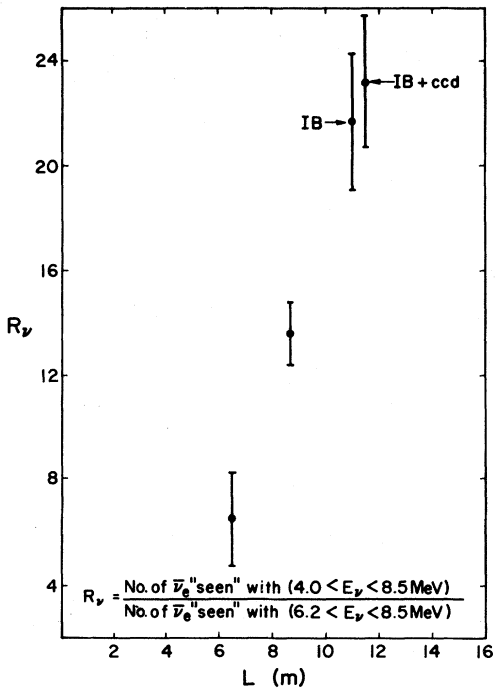

FIG. 2. Shown as a function of distance are the values of R_ν [defined in Eq. (7.1)] deduced from the individual fits [Eq. (5.1)]. For the 11.2-m experiments the data point marked IB is for the IB experiment alone obtained by using the last fit in Eq. (5.1) and the data point marked (IB + ccd) uses the best fit [Eq. (6.4)] to the data from the IB and the ccd measurement in the deuteron experiment at that distance.

VII. DISTANCE DEPENDENCE EXHIBITED BY THE MEASURED $\bar{\nu}_e$ SPECTRA

A. Two-bin analysis

The $\bar{\nu}_e$ spectra "seen" through the IB experiments at 6.5, 8.7, and 11.2 m exhibit a trend, see Fig. 1. For $E_\nu \gtrsim 6$ MeV the $\bar{\nu}_e$ spectrum at 6.5 m is the highest, that at 11.2 m is the lowest, and the 8.7-m spectrum lies between those two. For $E_\nu \lesssim 6$ MeV that ordering is reversed.

To statistically analyze this trend we divide the overlapping energy range $4<E_\nu<8.5$ MeV of the three experiments into two halves (bins) and integrate each of these spectra for the intervals $4<E_\nu<6.2$ MeV and $6.2<E_\nu<8.5$ MeV. The statistical uncertainties on these integrated rates will be less than on individual data points. To remove the normalization uncertainties, which comprise a significant fraction of the errors on each of the measured spectra, we take the ratio R_ν of the two bins at each distance plus one (or total/upper bin):

$$R_\nu = \frac{\text{No. of } \bar{\nu}_e \text{ "seen" with } (4 < E_\nu < 8.5 \text{ MeV})}{\text{No. of } \bar{\nu}_e \text{ "seen" with } (6.2 < E_\nu < 8.5 \text{ MeV})} \ . \tag{7.1}$$

We find the results (with statistical and energy-calibration errors, respectively)

$$\begin{aligned}
&6.5 \text{ m expt} \rightarrow R_\nu = 6.6 \pm 1.8 \pm 0.24 = 6.6 \pm 1.8 \ , \\
&8.7 \text{ m expt} \rightarrow R_\nu = 13.61 \pm 0.87 \pm 0.80 = 13.6 \pm 1.2 \ , \\
&11.2 \text{ m (IB only) expt} \rightarrow R_\nu = 21.70 \pm 0.90 \pm 2.40 = 21.7 \pm 2.6 \ , \\
&\overline{11.2 \text{ m}} \text{ (IB + ccd) expts} \rightarrow R_\nu = 23.2 \pm 1.0 \pm 2.3 = 23.2 \pm 2.5 \ .
\end{aligned}$$

In Fig. 2 we show the distance dependence exhibited by the measured values of R_ν at the three distances. In terms of relative standard deviations for the differences

$$\begin{aligned}
&(\Delta R_\nu)_{8,11} = 2.9 \text{ SD}, \quad (\Delta R_\nu)_{6,8} = 3.2 \text{ SD}, \quad (\Delta R_\nu)_{6,11} = 4.8 \text{ SD} \ , \\
&(\Delta R_\nu)_{8,\overline{11}} = 3.5 \text{ SD}, \quad (\Delta R_\nu)_{6,\overline{11}} = 5.7 \text{ SD} \ ,
\end{aligned} \tag{7.2}$$

where $\overline{11}$ refers to the spectral fit (6.4) to 11.2-m IB and ccd together.

Indeed such a distance dependence is exhibited by the measured e^+ spectra themselves. From the IB experiments we can directly deduce the number of e^+ observed in the corresponding (recall $E_\nu = E_e + 1.8$ MeV) intervals: $(2.2 < E_e < 6.7$ MeV) and $(4.4 < E_e < 6.7$ MeV). We find that the ratio

$$R_e = \frac{\text{No. of } e^+ \text{ observed in the interval } 2.2 < E_e < 6.7 \text{ MeV}}{\text{No. of } e^+ \text{ observed in the interval } 4.4 < E_e < 6.7 \text{ MeV}} \tag{7.3}$$

equals (again, statistical plus energy-calibration errors)

$$\begin{aligned}
&R_e = 3.3 \pm 0.68 \pm 0.08 = 3.3 \pm 0.68 \quad (6.5 \text{ m}) \ , \\
&R_e = 5.90 \pm 0.50 \pm 0.22 = 5.9 \pm 0.55 \quad (8.7 \text{ m}) \ , \\
&R_e = 8.37 \pm 0.35 \pm 0.71 = 8.4 \pm 0.78 \quad (11.2 \text{ m}) \ .
\end{aligned} \tag{7.4}$$

Thus (see Fig. 3)

$$(\Delta R_e)_{8,11} = 2.6 \text{ SD}, \quad (\Delta R_e)_{6,8} = 3.0 \text{ SD}, \quad (\Delta R_e)_{6,11} = 4.9 \text{ SD} \ . \tag{7.5}$$

Since the detectors at the three distance had somewhat different energy-dependent detection efficiencies, the ratios R_e thus extracted do not represent a precise comparison of the three spectra. The R_ν ratios calculated from the spectral fits (5.1) via (2.4) provide a more accurate comparison of the spectra monitored at the three distances.

B. Implications of the $\bar{\nu}_e$ spectra measured at different distances for the deuteron rates measured at 11.2 m

The $\bar{\nu}_e$ spectra measured via the IB experiment at 6.5, 8.7, and 11.2 m allow one to calculate the rates [Γ(ccd) and Γ(ncd)] for charged- and neutral-current disintegration of the deuteron at that particular distance. The differences between the ccd and ncd rates [and/or their ratio, $r_d = \Gamma(\text{ccd})/\Gamma(\text{ncd})$] measured at 11.2 m and that implied by the measured $\bar{\nu}_e$ energy spectra at 6.5 and 8.7 m constitute a deviation from the no-oscillation hypothesis. We find for the event rates per day using the covariance matrix from the spectral fits for statistical errors:

$$6.5 \text{ m} \rightarrow \begin{cases}
\Gamma(\text{ccd})_6 = 113[\pm 41\%(\text{statistical}) \pm 10\%(\text{systematics}) \pm 8.7\%(\text{calibration})] = 113 \pm 49 \ , \\
\Gamma(\text{ncd})_6 = 185(\pm 23\% \pm 10\% \pm 6.9\%) = 185 \pm 26 \ , \\
r_6 = \Gamma(\text{ccd})_6/\Gamma(\text{ncd})_6 = 0.61 \pm 0.10 \ ,
\end{cases} \tag{7.6}$$

$$8.7\text{ m}\rightarrow\begin{cases}\Gamma(\text{ccd})_8=52.4(\pm5.4\%\pm8\%\pm11.5\%)=52.4\pm7.9\ ,\\ \Gamma(\text{ncd})_8=138.8(\pm3.1\%\pm8\%\pm7.8\%)=139\pm16\ ,\\ r_8=0.378\pm0.018\ ,\end{cases}\tag{7.7}$$

experimental:

$$11.2\text{ m}\rightarrow\begin{cases}\overline{\Gamma}(\text{ccd})_{11.2}=37.3\pm8.0,\quad \Gamma(\text{ncd})_{11.2}=165\pm25\ ,\\ \bar{r}_{11.2}=\overline{\Gamma}(\text{ccd})_{11.2}/\Gamma(\text{ncd})_{11.2}=0.226\pm0.059\ .\end{cases}\tag{7.8}$$

If there are no neutrino oscillations then the numbers for Γ(ccd), Γ(ncd), or $r_d=\Gamma(\text{ccd})/\Gamma(\text{ncd})$ should be independent of distance. We see that the three values for Γ(ncd) given above are within about 1 SD of each other whereas those for Γ(ccd) and for r_d are appreciably different at different distances.

In statistically analyzing these differences, use of the ratio $r_d=\Gamma(\text{ccd})/\Gamma(\text{ncd})$ rather than Γ(ccd) or Γ(ncd) has some advantages because the normalization uncertainties in the measured $\bar{\nu}_e$ spectra cancel. In addition the error in Γ(ccd) or Γ(ncd) due to the e^+ energy-calibration uncertainty is much more than on the ratio r_d. Also the statistical errors on the ratio are somewhat smaller than on Γ(ccd) or Γ(ncd). Figure 4 presents a comparison of r_d for the three distances. For the difference between the values of r_d implied by the 6.5-m experiment and that measured at 11.2 m we use the notation $(\Delta r)_{6,11}$. Thus

$$\begin{aligned}(\Delta r)_{6,11}&=3.3\text{ SD}\ ,\\ (\Delta r)_{8,11}&=2.5\text{ SD}\ .\end{aligned}\tag{7.9}$$

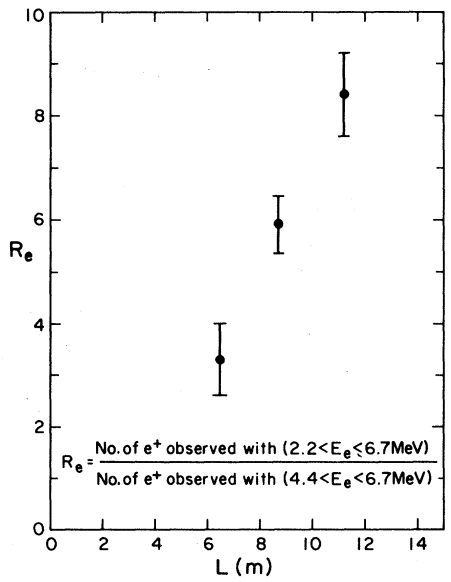

FIG. 3. Shown as a function of distance are the measured values of R_e [defined in Eq. (7.3)] deduced directly from the observed e^+ histograms.

C. Multibin analysis

We now perform a χ^2 fit to all available data bins from three experiments for a nonoscillating neutrino spectrum. The data are as follows.

(1) From the 8.7-m experiment we use 19 data points in the interval $1.0\lesssim E_e\lesssim 6.7$ MeV, with normalization uncertainty on η_{s8} of 8%, and calibration uncertainty on ϵ_8 of 2%, i.e., altogether 21 data points $[E_e^{\text{true}}=(1+\epsilon)E_e^{\text{meas}}]$.

(2) From the 11.2-m experiment we use 9 data points in the energy interval $2.5\lesssim E_e\lesssim 7.0$ MeV, with η_{s11} ($\pm14\%$) and ϵ_{11} ($\pm2.5\%$), i.e., altogether 11 data points.

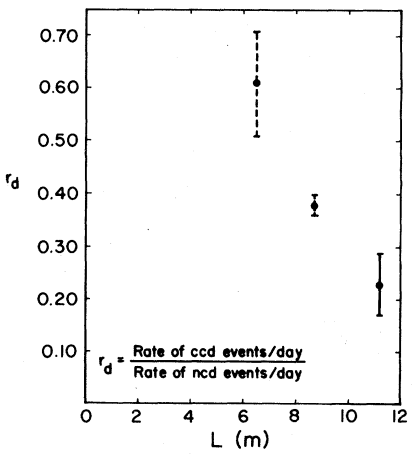

FIG. 4. Shown are the values (dashed) of the ratio $r_d=\Gamma(\text{ccd})/\Gamma(\text{ncd})$ implied by the 6.5- and 8.7-m IB experiments and the weighted mean for $\Gamma(\text{ccd})/\Gamma(\text{ncd})$ at 11.2 m obtained from the deuteron experiment and that implied by the IB experiment.

(3) From the deuteron-disintegration experiment performed at 11.2 m we use the ncd rate of (165 ± 25)/day and the ccd rate of (28 ± 12)/day as two more data points.

We start by searching for a no-oscillation joint spectrum of the form (3.1) that is best able to account for the 15 data points from the 8.7-m experiment that overlap with the ones in the 11.2-m experiment lying in the energy range $4.0<E_\nu<8.5$ MeV. In addition the ccd measured rate which has a threshold in the corresponding energy interval $E_\nu>4$ MeV is included whereas the ncd measured rate is not included because its threshold is $E_\nu=2.5$ MeV which is below the energy spectrum measured at 11.2 m. So altogether 29 data points are used (data set No. 1) and the no-oscillation best fit has

$$\chi^2/d_f=33.6/19\rightarrow\text{C.L.}=0.021\ .$$

The parameters of this fit are $(A_0,\ldots,A_5)$

$$0.56, 0.756, -0.5452\ ,$$

$$0.071\,67, -0.002\,319, -0.000\,190\,5$$

with $\eta_{s8}=0.98$, $\eta_{s11}=1.14$, $\epsilon_8=-0.022$, $\epsilon_{11}=0.032$.

We next use only the 8.7 and 11.2 m IB experiments. Once again only the overlapping data points in the energy interval $4\lesssim E_\nu\lesssim8.5$ MeV are included (data set No. 2). So altogether there are 28 points in this analysis and the best no-oscillation fit gives

$$\chi^2/d_f=31.3/18\rightarrow\text{C.L.}=0.026\ .$$

The parameters are almost identical to those for the fit with ccd given above.

In Table I we present a summary of the confidence levels of the no-oscillations fits discussed above. We note that the no-oscillation best fits to reactor data (with or without the 6.5-m experiment) have C.L. <0.026. The ccd/ncd ratio implied by this fit is 0.33 which is 1.7 SD from the weighted mean of its measured value of 0.23 ± 0.06.

D. Energy-calibration and energy-resolution effects on the joint no-oscillation fits

Since the spectrum measured at 11.2 m is much steeper (for $E_\nu\gtrsim5$ MeV) than the ones measured at 6.5 and 8.7 m it is therefore quite sensitive to e^+ energy calibration and energy resolution. We thus study the effect of varying these parameters on the joint no-oscillation fits to data set No. 1 (8, 11 overlap and ccd) and data set No. 2 (8, 11 overlap).

We first relax the energy-calibration uncertainty $\sigma_{\epsilon_{11}}$ for the 11.2-m experiment to 5% from its stated value of 2.5%. We find then that the best no-oscillation fits for data set No. 1 ($\Delta\epsilon\equiv\epsilon_{11}-\epsilon_8$) are

$$\chi^2/d_f=31.4/19\rightarrow\text{C.L.}=0.037\ \ (\sigma_{\epsilon_{11}}=0.05)\ ,$$

$$\epsilon_8=-0.014,\ \epsilon_{11}=0.052\ ,\ \ \Delta\epsilon=0.066$$

and for data set No. 2,

$$\chi^2/d_f=28.3/18\rightarrow\text{C.L.}=0.057\ ,$$

$$\epsilon_8=-0.010,\ \epsilon_{11}=0.055\ ,\ \ \Delta\epsilon=0.065\ .$$

We next study the extreme case with $\sigma_{\epsilon_{11}}$ relaxed to $\pm20\%$. We find for data set No. 1

$$\chi^2/d_f=30.1/19\rightarrow\text{C.L.}=0.05\ \ (\sigma_{\epsilon_{11}}=0.20)\ ,$$

$$\epsilon_8=-0.012,\ \epsilon_{11}=0.054\ ,\ \ \Delta\epsilon=0.066$$

and for data set No. 2

$$\chi^2/d_f=27.1/18\rightarrow\text{C.L.}=0.078\ ,$$

$$\epsilon_8=-0.006,\ \epsilon_{11}=0.066\ ,\ \ \Delta\epsilon=0.072\ .$$

For comparison we restate here the results with the experimental 2.5% uncertainty for data set No. 1,

$$\chi^2/d_f=33.6/19\rightarrow\text{C.L.}=0.021\ \ (\sigma_{\epsilon_{11}}=0.025)\ ,$$

$$\epsilon_8=-0.022\ ,\ \ \epsilon_{11}=0.032\ ,\ \ \Delta\epsilon=0.054$$

and for data set No. 2,

$$\chi^2/d_f=31.3/18\rightarrow\text{C.L.}=0.026\ ,$$

$$\epsilon_8=-0.017\ ,\ \epsilon_{11}=0.039\ ,\ \ \Delta\epsilon=0.056\ .$$

By comparing these fits we will find whether or not the energy-calibration errors are effectively restricting the confidence levels of the no-oscillation fits to small values. Since only the 8.7-m and 11.2-m IB spectra are being compared here, relaxing one energy calibration ($\sigma_{\epsilon_{11}}$) has the same net effect as relaxing the other or both together. We find that with the given experimental uncertainties a relative calibration shift $\Delta\epsilon$ of 5.4% is sought but with a total relaxation to 20% uncertainty the best fit still seeks only a 7.2% relative shift, and apportions itself to minimize χ^2.

We also find that relaxing the calibration beyond 5% only changes the χ^2 by reducing the penalty for the same energy shift, not by improving the fit in any other way. Thus the energy-calibration con-

straint does not significantly contribute to the low confidence level of the best no-oscillation fit and an underquote of the energy-calibration uncertainty by either experiment could not realistically increase the C.L. from 0.026 to more than 0.065.

We next examine the effect of sharpening the energy resolution of the 11.2-m experiment by varying it by 25% to $\sigma_{11}=0.145(E_{\rm obs}/{\rm MeV})^{1/2}$. For the best no-oscillation fits we then have data set No. 1:

$$\chi^2/d_f=30.8/19\rightarrow \text{C.L.}=0.043\ ,$$

data set No. 2:

$$\chi^2/d_f=28.4/18\rightarrow \text{C.L.}=0.057\ .$$

Thus even a substantial relaxation in the e^+ energy-calibration uncertainty or in the energy resolution leaves the confidence levels of the best no-oscillation fits to the IB experiments at 8.7 and 11.2 m to CL <0.10 with or without the ccd measurement at 11.2 m.

VIII. ANTINEUTRINO SPECTRAL RANGE FROM INVERSION OF MEASURED e^- SPECTRA

The measurements[7,8] of the reactor e^- spectra allow limits to be set on the reactor $\bar{\nu}_e$ spectra.[23,24] We now describe that process.[7]

The β^- decay spectra of both e^- and $\bar{\nu}_e$ from a given nuclear decay are uniquely determined by the end-point energy E and the Z of the final nucleus. Z enters through the Coulomb distortion of the final electron wave function which is embodied in the Fermi Coulomb function $F(Z,p_\beta)$. For a given Z there is a unique inversion of the e^- spectrum into the $\bar{\nu}_e$ spectrum. The problem in inverting the actual e^- spectra from fission is that many different Z contribute, centered about two peaks at $Z=36\pm4$ and $Z=55\pm5$. Since the higher-energy neutrinos arise from only a few percent of the decays it is reasonable to consider any Z that could produce a few percent of the decays and this gives a lower limit of $Z=32$ and an upper limit of $Z=60$ to be used in the Coulomb function. This will then give a range for inverted $\bar{\nu}_e$ spectra involving no assumptions of theoretically calculated spectra. The limits of the range will then be taken at 0.5-MeV intervals and given a 1-SD weighting in fitting the inverted e^- spectral data along with the IB and deuteron experiments. The procedure for inversion follows that of Carter, Reines, Wagner, and Wyman (Ref. 7, Appendix II). We proceed in two stages. First we fit the e^- spectra to a single exponential (average 3% accuracy $E_\nu=2$ to 7 MeV) and invert it analytically to find the Z dependence of the resulting $\bar{\nu}_e$ spectra as a percent deviation from the central Z value $Z=46$. The output is rather linear in Z. This approximate inversion using a single exponential actually agrees with the ILL inversion[8] to within 4% for $E_\nu=2$ to 6.5 MeV. In the second stage, to obtain higher accuracy, we take the ILL inversion (in which they used 25 fitted $\beta-$decay functions, one for each data point) and apply the percentage Z range to get the final range of the inverted $\bar{\nu}_e$ spectra.

We now describe the inversion technique for a given Z. For a given end-point energy E the decay distribution shape in electron energy E_β is given by

$$f(E,E_\beta,Z)=E_\beta^2(E-E_\beta)^2G(E_\beta,Z)\ , \tag{8.1}$$

where

$$G(E_\beta,z)=(p_\beta/E_\beta)F(Z,E_\beta)\ , \tag{8.2}$$

F is the Fermi Coulomb function, and $B(E,Z)$ is the normalization function

$$B^{-1}(E,Z)=\int_{m_e}^{E} f(E,E_\beta,Z)dE_\beta\ . \tag{8.3}$$

Letting $n(E,Z)$ be the end-point energy distribution the e^- spectrum for a given Z is then

$$Y(E_\beta)=E_\beta^2\int_{E_\beta}^{\infty} dE\, n(E,Z)B(E,Z) \times G(E_\beta,Z)(E-E_\beta)^2 \tag{8.4}$$

and the $\bar{\nu}_e$ spectrum is

$$\rho(E_\nu,Z)=E_\nu^2\int_{E_\nu+m_e}^{\infty} dE\, n(E,Z)B(E,Z) \times G(E-E_\nu,Z)(E-E_\nu)^2\ . \tag{8.5}$$

Given the experimentally measured $Y(E_\beta)$ electron spectrum or a fit to it, we can invert it by first taking third derivatives of the solely E_β-dependent part to remove the integration,

$$-\frac{1}{2}\frac{d^3}{dE_\beta^3}\left[\frac{Y(E_\beta)}{E_\beta^2G(E_\beta,Z)}\right]=n(E_\beta,Z)B(E_\beta,Z)\ . \tag{8.6}$$

We then substitute this into (8.5) for $E_\beta=E$ and calculate $\rho(E_\nu,Z)$ for the given Z.

We fit the ILL data[8] for $Y(E_\beta)$ from ^{235}U fission with a single exponential for the range $E_\beta=2$ to 7 MeV with an average error of 3%,

$$Y(E_\beta)=E_\beta^2(5.75)\exp(-bE_\beta)\ , \tag{8.7}$$

where $b=1.475\ \mathrm{MeV}^{-1}$. To a good approximation we use[15]

$$G(E-E_\nu,Z)=G_m(Z)\exp[-c(E-E_\nu-m)^{1/2}]\ , \tag{8.8}$$

where $c=(0.216-0.007Z)/\sqrt{m}$ and the constant $G_m(Z)$ cancels out later. Substituting (8.7) and (8.8) into (8.6) and then into (8.5) gives explicitly the predominant E_ν dependence

$$\rho(E_\nu)=E_\nu^2(5.75)e^{-b(E_\nu+m)}e^{c\sqrt{E_\nu}}I(E_\nu,Z)\ , \tag{8.9}$$

where $I(E,Z)$ is a slowly varying integral function of E_ν and is evaluated numerically (it varies at most 10% at $Z=60$ over the range $E_\nu=2$ to 7.5 MeV),

$$I(E_\nu)=\int_0^\infty dE'(E'+m)^2\exp\{-bE'+c[(E_\nu+E')^{1/2}-\sqrt{E_\nu}-\sqrt{E'}]\}\times\left[1-\frac{3c}{2b}(E_\nu+E')^{-1/2}-\frac{3c}{b^2}(E_\nu+E')^{-3/2}\right]. \tag{8.10}$$

The inversion (8.9) agrees with that of ILL to within 4% from $E_\nu=2$ to 6.5 MeV. Our inversion is accurate enough to calculate the percentage neutrino spectral range from $Z=32$ to $Z=60$ which varies from $\pm4\%$ at $E_\nu=3$ MeV to $\pm19\%$ at $E_\nu=7$ MeV centered about $Z=46$. The Z dependence is highly linear and $Z=46$ agrees with the average of the $Z=36$ and $Z=55$ peak centers. These percentage errors are applied to the ILL spectrum (which is only slightly shifted from the central $Z=46$) since that spectrum was inverted with more accuracy (25 β-decay functions instead of the two parameters above). To this are added in quadrature the 1.5% shape and 4% inversion errors. These limits are shown in Fig. 5 as dashed lines. Not shown is the 5% overall normalization uncertainty.

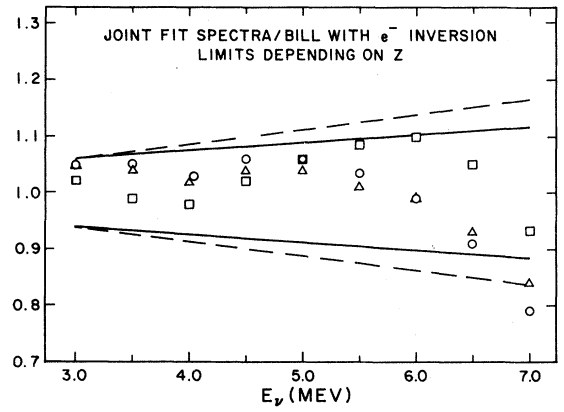

FIG. 5. The allowed range of the reactor $\bar{\nu}_e$ spectrum, obtained by inversion of the e^- spectrum measured by Refs. 7 and 8 is shown for limits of $Z=32$ and $Z=60$ (dashed) and for Z peaks at 36 and 55 (solid). The central values of the $\bar{\nu}_e$ spectrum extracted under the oscillation hypothesis for $\delta m^2=0.9$, 2.3, 3.7 eV^2 solutions are shown (□,△,○, respectively) for $E_\nu=3.0$, 3.5, . . . , 7.0 MeV as ratios to the central values of the spectrum obtained by inversion in Ref. 8.

We should elaborate here on the difference between the Schreckenback *et al.*[8] inversion and our range of inversion limits. Although only a few percent of the β-decay $\bar{\nu}_e$ are in the overlap energy range of the IB experiments, they assume that the split between the high- and low-Z peaks is at most $\frac{2}{3}$ and $\frac{1}{3}$. Because of the linearity in Z deviation the sum of these yields at most a $\frac{1}{3}$ deviation. Realizing that the small percentage of all $\bar{\nu}_e$'s that are at high energy could come totally from either peak would immediately *triple* their Z range away from the average Z. Rather than taking the peak centers $Z=36$ and $Z=55$ or $\Delta Z=19$ we took the range to include all Z that could give the $E_\nu\geq4$-MeV neutrinos, i.e., $Z=32$ to $Z=60$ or $\Delta Z=28$. Having taken only the peak centers would have reduced our range by $\frac{19}{28}\simeq\frac{2}{3}$. This peak-to-peak range is shown in Fig. 5 by solid lines. We note that the oscillation fits constrained by the inversion (see Sec. X) lie within that peak-to-peak Z range.

IX. NEUTRINO MIXING AND OSCILLATIONS (REFS. 25–29)

If neutrinos have mass and the masses are not identical, then the neutrinos associated with given leptons via the charged-current weak interactions ν_α ($\alpha=e,\mu,\tau$) (often called flavor eigenstates) may be mixtures of nondegenerate mass eigenstates ν_i ($i=1,2,3$). This is in fact the case in the quark sector between the flavor eigenstates d',s',b' and the mass eigenstates d,s,b. These eigenstates are connected with each other by a unitary transformation matrix U_{ai} involving four independent parameters[27] in the three-neutrino case and one in the

two-neutrino case,

$$|\nu_\alpha(0)\rangle=\sum_i U_{\alpha i}|\nu_i(0)\rangle\ . \tag{9.1}$$

If the energy and momentum of the emitted neutrino would be precisely determined observables in a given experiment in which flavor α was emitted, then for $(E_\nu{}^2-p_\nu{}^2)^{1/2}$ the mass eigenstates ν_i with eigenvalues $m_i=(E_\nu{}^2-p_\nu{}^2)^{1/2}$ would be projected out with probabilities $|U_{\alpha i}|^2$.

In oscillation experiments the resolutions are so large on the scale of possible neutrino masses that the m_i are not observables but only another (or the same) flavor state ν_β is projected out. In contrast in the tritium-decay experiment[30] the expectation value of the Hamiltonian can be measured:

$$\begin{aligned}\text{“}m_{\nu_\alpha}\text{”}&\equiv\langle\nu_\alpha(0)|H|\nu_\alpha(0)\rangle\\&=\sum_i|U_{\alpha i}|^2m_i\ .\end{aligned} \tag{9.2}$$

We now consider the oscillation experiments detecting a flavor β a distance L from where a flavor α was emitted. For energies of the order of MeV or greater and neutrino masses of the order of eV there is obviously going to be no difference in wave-packet coefficients or momentum-space probabilities for the different mass states so we can analyze each component separately. The oscillation result, which is very slowly varying over the ΔE or Δp width of the packet, will then be true for the whole packet. A detailed analysis of packets has been done by Kayser[31] verifying this. For simplicity we work with states of the same energy but a superposition of different mass states of momenta $p_i=(E^2-m_i{}^2)^{1/2}$. Plane-wave mass eigenstates created at $z=0$, $t=0$, $|\nu_i(0,0)\rangle$, propagate as

$$|\nu_i(z,t)\rangle=e^{i(Et-p_iz)}|\nu_i\rangle\ . \tag{9.3}$$

The original superposition created by the weak charged current is

$$|\nu_\alpha\rangle=\sum_i U_{\alpha i}|\nu_i\rangle\ . \tag{9.4}$$

At z,t the superposition now has phases

$$|\nu_\alpha(z,t)\rangle=e^{iEt}\sum U_{\alpha i}e^{-ip_iz}|\nu_i\rangle\ . \tag{9.5}$$

The amplitude for detecting the neutrino with flavor β is obtained by projecting this into the superposition (9.1) for $|\nu_\beta\rangle$,

$$\langle\nu_\beta|\nu_\alpha(z,t)\rangle=e^{iEt}\sum_i U_{\alpha i}U^*_{\beta i}e^{-ip_iz}\ . \tag{9.6}$$

The probability is then

$$P_{\alpha\to\beta}(z)=\sum_{ij}U_{\alpha i}U^*_{\beta i}U^*_{\alpha j}U_{\beta j}e^{i(p_j-p_i)z}\ . \tag{9.7}$$

For direct detection where $\beta=\alpha$, taking terms in pairs

$$P_{\alpha\to\alpha}(z)=\sum_i|U_{\alpha i}|^4+2\sum_{i<j}|U_{\alpha i}|^2|U_{\alpha j}|^2\cos(p_j-p_i)z\ . \tag{9.8}$$

For $E\gg m_i$,

$$p_j-p_i\simeq\frac{m_i{}^2-m_j{}^2}{2E}=\frac{\delta m^2{}_{ij}}{2E}\ .$$

For δm^2 in $(\text{eV})^2$, E in MeV, and $z=L$ in meters,

$$P_{\alpha\to\alpha}(L)=\sum_i|U_{\alpha i}|^4+2\sum_{i<j}|U_{\alpha i}|^2|U_{\alpha j}|^2\cos\left[\frac{2.53\delta m^2{}_{ij}L}{E}\right]\ . \tag{9.9}$$

For two-neutrino mixing, $U_{\alpha1}=\cos\theta$, $U_{\alpha2}=\sin\theta$, $U_{\beta1}=-\sin\theta$, $U_{\beta2}=\cos\theta$, this converts to the familiar form

$$P_{\alpha\to\alpha}(L)=1-\sin^22\theta\sin^2\left[\frac{2.53\delta m^2L}{2E}\right]\ . \tag{9.10}$$

For transitions $\alpha\neq\beta$, Eq. (9.7) becomes

$$\begin{aligned}P_{\alpha\to\beta}(L)=&-4\sum_{i<j}\mathrm{Re}(U_{\alpha i}U^*_{\beta i}U^*_{\alpha j}U_{\beta j})\sin^2\left[\frac{2.53\delta m^2{}_{ij}L}{2E}\right]\\&-2\sum_{i<j}\mathrm{Im}(U_{\alpha i}U^*_{\beta i}U^*_{\alpha j}U_{\beta j})\sin\left[\frac{2.53\delta m^2{}_{ij}L}{E}\right]\ .\end{aligned} \tag{9.11}$$

The sine terms proportional to imaginary parts that violate CP (Ref. 32) give the differences $(P_{\alpha\to\beta}-P_{\beta\to\alpha})$ and can be shown for the 3ν case to be equal in magnitude for all $\alpha\neq\beta$, giving only one *CP*-violation parameter. For antineutrinos use U^* above for U.

For two neutrinos, no phases occur and this becomes for transitions

$$P_{\alpha\to\beta}=P_{\beta\to\alpha}=\sin^2 2\theta\sin^2\left[\frac{2.53\delta m^2 L}{2E}\right]. \tag{9.12}$$

The form (9.9) is useful since the long-distance average is given by the first term, and the source or detector size directly damps the cosine terms (see Appendix).

It should be noted that in analyzing experiments in only a single direct channel (as in this report $\bar{\nu}_e\to\bar{\nu}_e$) for three neutrinos oscillating, if the neutrino masses are ordered $m_3<m_2<m_1$ then the fits will have a twofold ambiguity or symmetry under the interchange $\delta m^2{}_{12}\leftrightarrow\delta m^2{}_{23}$ with $|U_{e1}|^2\to|U_{e3}|^2$ as can be seen from Eq. (9.9).

Pseudo-2ν cases (two relatively near masses)

In general the masses m_1,m_2,m_3 may all be the same order but not relatively close to each other. In that case all terms in Eqs. (9.9) and (9.12) will give distinct oscillation lengths, constrained only by the identity

$$\delta m^2{}_{12}+\delta m^2{}_{23}+\delta m^2{}_{31}=0\,. \tag{9.13}$$

It is also likely, especially if neutrino masses are staged like lepton or current quark masses, that two of the masses are relatively close, say m_2 and m_3. This would give then

$$|\delta m^2{}_{23}|\ll\delta m^2{}_{12},\delta m^2{}_{13}.$$

1. *High-δm^2 detection*

In a sequence of experiments the larger-δm^2 oscillations might be detected first with the two terms in $\delta m^2{}_{12}\simeq\delta m^2{}_{13}$ combining with the same oscillation length, and the very small $\delta m^2{}_{23}$ would not yet be causing oscillations in

$$\cos\left[\frac{2.53\delta m^2{}_{23}L}{E}\right],$$

but going into the constant. Thus we take

$$\delta m^2{}_{12}\simeq\delta m^2{}_{13}\equiv\delta m^2\,. \tag{9.14}$$

Recombining terms in (9.9) and (9.11) for this case gives for disappearance experiments

$$P_{\alpha\to\alpha}=1-4|U_{\alpha1}|^2(1-|U_{\alpha1}|^2)\times\sin^2\left[\frac{2.53\delta m^2 L}{2E}\right], \tag{9.15}$$

$$P_{\beta\to\beta}=1-4|U_{\beta1}|^2(1-|U_{\beta1}|^2)\times\sin^2\left[\frac{2.53\delta m^2 L}{2E}\right], \tag{9.16}$$

etc., and for flavor-appearance experiments

$$P_{\alpha\to\beta}=P_{\beta\to\alpha}=4|U_{\alpha1}|^2|U_{\beta1}|^2\times\sin^2\left[\frac{2.53\delta m^2 L}{2E}\right]. \tag{9.17}$$

This is to be contrasted with a true decoupling case where $U_{\gamma1}=0$, $U_{\gamma2}=0$, $U_{\gamma3}=1$ and the remaining 2×2 α-β matrix gives (9.10) and (9.12). In the pseudo-2ν cases above a *single* experiment of (9.15), (9.16), or (9.17) has the *form* of (9.10) or (9.12) but upon doing two or more experiments, it is found that a single $\sin\theta,\cos\theta$ does not account for all, since

$$|U_{\alpha1}|^2+|U_{\beta1}|^2=1-|U_{\gamma1}|^2\neq1\,. \tag{9.18}$$

So even before L/E is large enough that the smallest $\delta m^2{}_{23}$ can be seen oscillating, we may infer its presence from (9.18).

2. Low-δm^2 detection

Another possible pseudo-2ν case is where $\delta m^2{}_{12}\simeq\delta m^2{}_{13}\gg\delta m^2{}_{23}$ and it is $\delta m^2{}_{23}\equiv\delta m^2$ that is detected oscillating. In this case $\delta m^2{}_{12}\simeq\delta m^2{}_{13}$ provide oscillations that average out, i.e., are damped by the source or detector size (see Appendix) or by energy-resolution width. In the case that two of the terms in (9.9) are damped to zero we may use $|U_{\alpha1}|^2+|U_{\alpha2}|^2+|U_{\alpha3}|^2=1$ and rewrite this case as

$$P_{\alpha\to\alpha}=[|U_{\alpha1}|^4+(1-|U_{\alpha1}|^2)^2]\left[1-\frac{4|U_{\alpha2}|^2(1-|U_{\alpha1}|^2-|U_{\alpha2}|^2)}{|U_{\alpha1}|^4+(1-|U_{\alpha1}|^2)^2}\sin^2\left[\frac{2.53\delta m^2 L}{2E}\right]\right]. \tag{9.19}$$

TABLE I. Comparison of confidence levels for hypotheses.

No.	Data set	Oscillation solutions δm^2 (eV^2)	$\sin^2 2\theta$	χ^2 subset No. 1	χ^2 subset No. 2	χ^2/d_f	C.L.
Hypothesis: no oscillations							
(1)	8.7 m + 11.2 m (only overlapping data points)			31.3		31.3/18	(0.026)
(2)	8.7 m + 11.2 m (only overlapping data points) + ccd				33.6	33.6/19	(0.021)
Hypothesis: oscillations 2ν							
(3)	8.7 m + 11.2 m + ncd + ccd	0.94	0.38	25.8	29.1	31.2/22	(0.09)
		2.33	0.21	20.5	22.9	26.4/22	(0.24)
		3.72	0.29	22.4	24.4	25.8/22	(0.26)
(4)	8.7 m + 11.2 m + ncd + ccd + e^- inversion limits	0.95	0.32	27.1	29.7	33.8/32	(0.38)
		2.34	0.20	23.0	25.7	30.4/32	(0.55)
		3.75	0.25	24.7	27.0	30.8/32	(0.53)
Hypothesis: oscillations 3ν		δm^2_{ij} (eV^2)	$4U_{ei}^2U_{ej}^2$				
(5)	Same as (3)	0.8	0.27	16.5	19.1	23.4/20	(0.27)
		2.5	0.18				
		(3.3 or 1.7)	0.02				
(6)	Same as (4)	0.9	0.17	19.0	21.1	27.1/30	(0.60)
		2.4	0.16				
		(3.3 or 1.5)	0.01				

We note in this case that there is a depletion in the energy-independent overall normalization of detected neutrinos multiplying a standard 2ν oscillation formula. In the reactor experiments with $\bar{\nu}_e$ this pseudo-2ν form can only be distinguished from a decoupled form if a fairly exact value of the reactor $\bar{\nu}_e$ spectrum is independently known to test whether there is a coefficient $[\,|U_\alpha|^4 + (1-|U_{\alpha 1}|^2)^2]$ of the oscillation fit that differs from one. We analyze this case in Sec. XI, after the oscillation fits are presented. In the reactor experiments this case would apply for $\delta m^2_{13} \simeq \delta m^2_{12} > 10$ eV^2 for the small ILL reactor and > 3 eV^2 for the larger power reactors.

X. JOINT OSCILLATION 2ν SOLUTIONS TO REACTOR DATA

We now report the best 2ν flavor-oscillation fits to reactor data. In addition to the data points from the three experiments (disregarding the 6.5-m experiment) initiated by $\bar{\nu}_e$ we also include the data from the range of reactor $\bar{\nu}_e$ spectra obtained by inversion of the measured β spectrum. Ten data points with $2.5 \leq E_\nu \leq 7.0$ MeV for the range of inverted spectra plus the electron spectra normalization η_{se} with uncertainty of 5% are included (see Sec. VIII). Altogether the analysis includes 45 data points. There are three oscillation best fits to the reactor data. These have the following values for $(\delta m^2, \sin^2 2\theta)$:

$$\begin{aligned} &\text{(a) } (0.95 \text{ eV}^2, 0.32)\,, \\ &\quad \chi^2/d_f = 33.8/32, \quad \text{C.L.} = 0.38\,, \\ &\text{(b) } (2.34 \text{ eV}^2, 0.20)\,, \\ &\quad \chi^2/d_f = 30.4/32\,, \quad \text{C.L.} = 0.55\,, \\ &\text{(c) } (3.75 \text{ eV}^2, 0.25)\,, \\ &\quad \chi^2/d_f = 30.8/32\,, \quad \text{C.L.} = 0.53\,. \end{aligned} \tag{10.1}$$

The complete set of parameters corresponding to these 2ν oscillation solutions are given in Table II

TABLE II. Best fits with two-component neutrino oscillations. The data are from the 8.7- and 11.2-m IB, ccd, and ncd experiments and the reactor $\bar{\nu}_e$ spectrum implied by inversion of the measured e^- spectrum. The fits are up to 45 data points with 13 parameters.

δm^2 (eV^2)	0.95	2.34	3.75
$\sin^2 2\theta$	0.32	0.20	0.25
χ^2/d_f	33.8/32	30.4/32	30.8/32
C.L.	0.38	0.55	0.53
Parameters			
A_0	0.33	−0.36	−0.07
A_1	0.662	1.006	0.833
A_2	−0.452 7	−0.447 0	−0.440 3
A_3	0.045 69	0.025 76	0.038 79
A_4	0.001 664	0.004 000	0.001 420
A_5	−0.000 424 7	−0.000 476 5	−0.000 342 4
η_{s8}	1.04	1.01	1.02
η_{s11}	1.11	1.17	1.18
η_{se}	1.02	1.02	1.03
ϵ_8	−0.034	−0.016	−0.009
ϵ_{11}	0.034	0.047	0.041

and compared in 4 of Table I. Figure 6 shows the 90%-C.L. limits (solid lines) about each of these solutions. Our best values for the oscillation parameters are (90%-C.L. limits):

$$\begin{aligned}
&\text{(a) } \delta m^2 = 0.95 \pm 0.10 \text{ eV}^2 , \\
&\qquad \sin^2 2\theta = 0.32 \pm 0.11 , \\
&\text{(b) } \delta m^2 = 2.34 \pm 0.23 \text{ eV}^2 , \\
&\qquad \sin^2 2\theta = 0.20 \pm 0.07 , \\
&\text{(c) } \delta m^2 = 3.75 \pm 0.27 \text{ eV}^2 , \\
&\qquad \sin^2 2\theta = 0.25 \pm 0.08 .
\end{aligned} \tag{10.2}$$

We next disregard the constraint on the reactor $\bar{\nu}_e$ spectrum from the e^- β spectra of ^{235}U (see Table III). We search for joint fits to the remaining three experiments, i.e., 8.7 m, 11.2 m, and ccd and ncd [see Table II and (3) of Table I] and find the following oscillation (δm^2,$\sin^2 2\theta$) best-fit solutions:

$$\begin{aligned}
&\text{(a) } (0.94 \text{ eV}^2, 0.29) , \\
&\qquad \chi^2/d_f = 31.2/22 , \quad \text{C.L.} = 0.09 , \\
&\text{(b) } (2.33 \text{ eV}^2, 0.21) , \\
&\qquad \chi^2/d_f = 26.4/22, \quad \text{C.L.} = 0.24 , \\
&\text{(c) } (3.72 \text{ eV}^2, 0.29) , \\
&\qquad \chi^2/d_f = 25.8/22, \quad \text{C.L.} = 0.26 .
\end{aligned} \tag{10.3}$$

We may compare these confidence levels without the e^- spectral inversion [set (3) Table I] to the no-oscillation confidence level for similar data sets (1) and (2) in Table I. We see that the C.L. of the best oscillation solutions exceed that of the no-oscillation solutions by factors of up to 12.

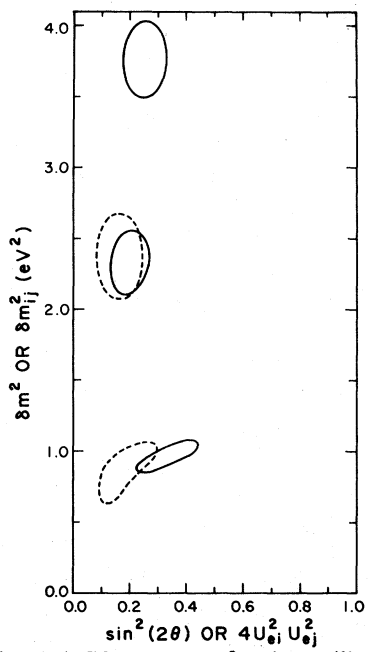

FIG. 6. 90%-C.L. contours for the oscillation parameters. The input data contain the IB experiments at 8.7 and 11.2 m, ncd and ccd rates measured in the deuteron experiment at 11.2 m, and the range for the reactor $\bar{\nu}_e$ spectra implied by inversion of the e^- spectrum from fission of ^{235}U. The allowed region (90% C.L.) lies inside of each contour. The three contours for the 2ν case are shown by solid lines. The oscillation-solution contours obtained under the 3ν hypothesis are shown by dashed lines.

TABLE III. Best fits with two-component neutrino oscillations. The data are from the 8.7- and 11.2- m IB, ccd, and ncd experiments. The fits are to 34 data points with 12 parameters.

δm^2 (eV^2)	0.94	2.33	3.72
$\sin^2 2\theta$	0.29	0.21	0.29
χ^2/d_f	31.2/22	26.4/22	25.8/22
C.L.	0.09	0.24	0.26
Parameters			
A_0	0.0	0.22	0.07
A_1	0.786	0.853	0.835
A_2	−0.456 4	−0.456 6	−0.443 1
A_3	0.045 71	0.028 46	0.038 30
A_4	0.001 281	0.004 548	0.001 453
A_5	−0.000 383 7	−0.000 556 3	−0.000 342 1
η_{s8}	1.03	0.97	0.97
η_{s11}	1.15	1.13	1.12
ϵ_8	−0.031	−0.027	0.97
ϵ_{11}	0.034	0.034	0.025

Another comparison is to find the decrease in χ^2 from the no-oscillation to the oscillation case for the same data set (1) or (2). From Table I we see that in general there is a reduction in χ^2 of 4 to 11 with the introduction of the two oscillation parameters despite the addition of four more data points [in data set (3)] to the overlapping data points of (1) or (2). With the additional constraint of the e^- inversion limits the reduction in χ^2 due to the two oscillation parameters is about 4 to 8 since an increase in χ^2 of about 2 to 4 arises from the extra 10 weakly constraining inversion data points.

As an important consistency check we solve for the reactor $\bar{\nu}_e$ spectrum in conjunction with each of our oscillation solutions given in Eq. (10.1). The resulting spectra are shown in Fig. 5 as ratios to the reactor $\bar{\nu}_e$ spectrum obtained[9] by inversion of the e^- spectrum. The errors on these spectra, estimated at about 5%, and the overall normalization uncertainty on the spectrum of Ref. 8 of 5% are not shown in the Figure. We note that the reactor spectra thus obtained lie within the solid lines which represent the restricted peak-to-peak range of $Z=36$ and $Z=55$ (see Sec. VIII).

In Fig. 7(a) and 7(b) we show the ratio $Y_{\text{exp}}/Y_{\text{spectrum}}$ (where Y_{exp} are the measured rates in 8.7- and 11.2-m experiments and Y_{spectrum} are the rates calculated on the basis of the reactor $\bar{\nu}_e$ spectra solved for in conjunction with our oscillation solutions and shown in Fig. 5) versus $\psi=2.53\,\delta m^2 L/E_\nu$ and compare that with the curve for the survival probability $P(L/E)$ from two-component oscillation theory. Figure 7(a) shows the 0.9-eV^2 solution and Fig. 7(b) the 2.3-eV^2 solution. For the latter the reactor size damping makes the $P(L/E)$ curves different for the 8.7- (solid) and the 11.2-m (dashed) experiments.

The 90%-C.L. contours for the oscillation parameters resulting from our joint analysis of reactor experiments is compared in Fig. 8 with the works of Boehm *et al.*[4] and that of RSP.[6] The allowed regions of Boehm *et al.*, resulting from their own analysis of their IB experiment at 8.7 m, lies to the left of the contours on the left (marked ILL). The allowed region of RSP, resulting from their own analysis of their ratio ccd/ncd measured in their deuteron experiment, lies to the right of the contours on the right (marked UCI). Our solutions obtained from joint analysis of reactor experiments, given in Eq. (10.2), are shown as darkly shaded. We note that our solutions are within the 68%-C.L. contour of Boehm *et al.* and are not incompatible with the RSP (90%-C.L.) contour.

XI. ANALYSIS OF PSEUDO-2ν CASE USING REACTOR EXPERIMENTS

A. Low δm^2 detected

The case of $\delta m^2_{13}=\delta m^2_{12}\gg\delta m^2_{23}\equiv\delta m^2\sim 1-5$ eV^2 has been presented in Sec. IX and yields the result

$$P_{e\to e}=[U_{e1}{}^4+(1-U_{e1}{}^2)^2]\left[1-\frac{4U_{e2}{}^2(1-U_{e1}{}^2-U_{e2}{}^2)}{U_{e1}{}^4+(1-U_{e1}{}^2)^2}\sin^2\left[\frac{2.53\delta m^2 L}{2E}\right]\right] . \tag{11.1}$$

The oscillation solutions for the reactor spectrum occur generally close to the center of the reactor e^- inversion bounds and therefore about 10% below the maximum possible reactor spectrum. This then sets a bound on the overall spectral reduction coefficient in (11.1) of

$$0.9\le[U_{e1}{}^4+(1-U_{e1}{}^2)^2]\le 1 . \tag{11.2}$$

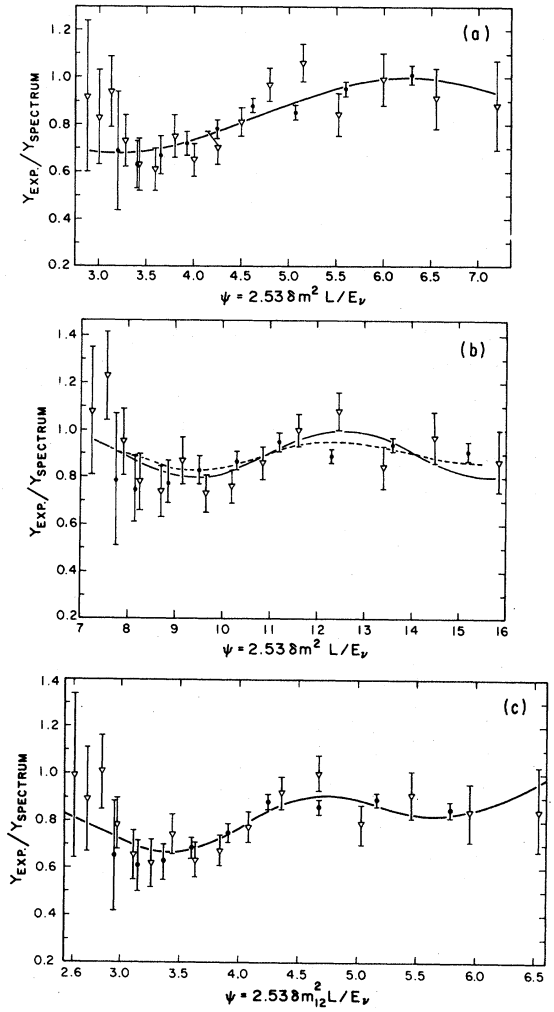

FIG. 7. $Y_{\rm exp}/Y_{\rm spectrum}$ vs ψ is compared with the survival probability $P(L/E)$ vs ψ. $Y_{\rm exp}$ is the measured rate and $Y_{\rm spectrum}$ is the rate expected from the zero-distance spectrum using the $\bar{\nu}_e$ spectra obtained under the oscillation hypothesis. Data marked ● are for the 11.2-m IB experiment. Data marked ∇ are for the 8.7-m experiment. (a) 2ν case, $\delta m^2=0.95$ eV^2; (b) 2ν case, $\delta m^2=2.33$ eV^2; (c) 3ν case, Eq. (12.3), where $\psi=2.53\delta m^2{}_{12}L/E$.

This has two possible solutions,

$$U_{e1}{}^2\ge 0.95 \quad \text{and} \quad U_{e1}{}^2\le 0.05 . \tag{11.3}$$

The coefficient of the oscillating term in (11.1) is $\sin^2 2\theta$ and using (11.2) as approximately 1 in this term gives

$$U_{e2}{}^2(1-U_{e1}{}^2-U_{e2}{}^2)=\frac{\sin^2 2\theta}{4} . \tag{11.4}$$

For the oscillation solutions with $0.03 \le(\sin^2 2\theta)/4\le 0.1$ the $U_{e1}{}^2\ge 0.95$ solution is not possible in (11.4). Then using the $U_{e1}{}^2\le 0.05$ solu-

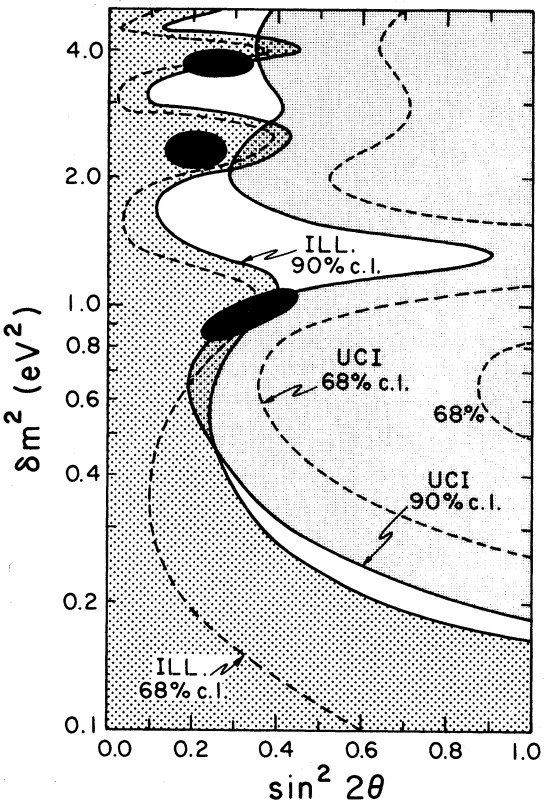

FIG. 8. Our 2ν oscillation solutions (darkly shaded) resulting from our joint analysis of reactor experiments are compared with the allowed regions of Boehm *et al.* (to the left of the contours on the left, resulting from their own analysis of their IB experiment at 8.7 m) and that of Reines *et al.* [to the right of the contours on the right, resulting from their own analysis of their ratio Γ(ccd)/Γ(ncd) measured in their deuteron experiment at 11.2 m]. Regions outside of our (darkly shaded) contours are excluded at the 90% C.L. Our 3ν oscillation solution is shown in Fig. 6.

tion in (11.2) we have from (11.4)

$$U_{e1}{}^2 \leq 0.05 ,$$
$$U_{e2}{}^2 = \frac{\sin^2 2\theta}{4} , \tag{11.5}$$
$$U_{e3}{}^2 = 1 - \frac{\sin^2 2\theta}{4} - U_{e1}{}^2 .$$

(Of course $U_{e2}{}^2$ and $U_{e3}{}^2$ can be interchanged here.)

Thus using reactor experiments alone we are able to show that the low-δm^2 pseudo-2ν case [which is very likely if "$m_{\nu e}$"$\simeq$30 eV (Ref. 30)] is restricted to two small electron mixing matrix elements.[33]

B. High δm^2 detected

If the high-δm^2 pseudo-2ν case applies, Eqs. (9.15) and (9.17), then the $\bar{\nu}_e \to \bar{\nu}_e$ reactor experiments give for the various δm^2 solutions

$$4 | U_{e1} |^2 (1 - | U_{e1} |^2) \simeq 0.1 \text{ to } 0.4 \tag{11.6}$$

which implies either

$$| U_{e1} |^2 \simeq 0.9 \text{ to } 0.97 \tag{11.7}$$

or

$$| U_{e1} |^2 \simeq 0.03 \text{ to } 0.1 . \tag{11.8}$$

XII. THREE-NEUTRINO OSCILLATION SOLUTIONS

We search for 3ν oscillation solutions to the reactor experiments which yield more than one distinct oscillation term, i.e., are distinct from the pseudo-2ν possibilities. We again disregard the 6.5-m experiment but include the constraint on the reactor $\bar{\nu}_e$ spectrum from inversion of the measured e^- spectrum. The analysis again includes 45 data points. The maximum-likelihood solution to the data has the following parameters with 90%-C.L. limits indicated:

$$U_{e1} = 0.95 \pm 0.02 ,$$
$$U_{e2} = 0.22 \pm 0.05 ,$$
$$U_{e3} = 0.21 \pm 0.05 ,$$
$$| \delta m^2_{12} | = 0.9 \pm 0.2 \text{ eV}^2 , \tag{12.1}$$
$$| \delta m^2_{13} | = 2.4 \pm 0.3 \text{ eV}^2 ,$$
$$\chi^2/d_f = 27.1/30 ,$$
$$\text{C.L.} = 0.60 .$$

The survival probability has the form [from Eq. (9.9)]

$$P_{\bar{\nu}_e \to \bar{\nu}_e} = 1 - 4 \sum_{i<j} | U_{ei} |^2 | U_{ej} |^2 \times \sin^2 \left[\frac{1.27 \delta m^2_{ij} L}{E} \right] . \tag{12.2}$$

The coefficients $4 | U_{ei} |^2 | U_{ej} |^2$ take the place in 3ν oscillations of the $\sin^2 2\theta$ in 2ν oscillations. For the above solution this becomes

$$P_{\bar{\nu}_e \to \bar{\nu}_e} = 1 - 0.17 \sin^2 \left[\frac{1.27(0.9)L}{E} \right] - 0.16 \sin^2 \left[\frac{1.27(2.4)L}{E} \right] - 0.01 \sin^2 \left[\frac{1.27 \delta m^2_{23} L}{E} \right] . \tag{12.3}$$

The contours of δm^2_{ij} vs $4 | U_{ei} |^2 | U_{ej} |^2$ can be represented on the same plot as δm^2 and $\sin^2 2\theta$. For the solution (12.1) and (12.3) the 90%-C.L. contours are shown (dashed) in Fig. 6. The 0.9- and 2.4-eV^2 terms contribute about the same but the third oscillating term is undetectable and allows two possibilities:

$$| \delta m^2_{23} | = (0.9 + 2.4 = 3.3) \text{ eV}^2$$

or

$$| \delta m^2_{23} | = (2.4 - 0.9 = 1.5) \text{ eV}^2 .$$

We next disregard the constraint on the reactor $\bar{\nu}_e$ spectrum from the fission e^- spectrum. The solution for the remaining 8.7 m, 11.2 m, ccd and ncd experiments has the parameters

$$U_{e1} = 0.93 ,$$
$$U_{e2} = 0.28 ,$$
$$U_{e3} = 0.23 ,$$
$$| \delta m^2_{12} | = 0.8 \text{ eV}^2 , \tag{12.4}$$
$$| \delta m^2_{13} | = 2.5 \text{ eV}^2 ,$$
$$\chi^2/d_f = 23.4/20 ,$$
$$\text{C.L.} = 0.27 ,$$

with $| \delta m^2_{23} | = 3.3$ or 1.7 eV^2.

The survival probability has the form

$$P_{\bar{\nu}_e\to\bar{\nu}_e}=1-0.27\sin^2\left[1.27(0.8)\frac{L}{E}\right]$$
$$-0.18\sin^2\left[1.27(2.5)\frac{L}{E}\right]$$
$$-0.02\sin^2\left[1.27\delta m^2{}_{23}\frac{L}{E}\right]. \quad (12.5)$$

The confidence levels for the 3ν solutions are presented in Table I for comparison with the no-oscillation and 2ν oscillation solutions. From Table I we see that with the introduction of four oscillation parameters in the 3ν case for data sets No. (1) or No. (2) there is a reduction in χ^2 of about 12 for the solution with e^- inversion constraints and of about 15 for the solution without those constraints.

In comparing the confidence levels for the 3ν oscillation solution with the 2ν solutions one finds an improvement in C.L. by about a factor of 3 over the 0.9-eV^2 2ν solution. The confidence levels for the 2.3- and 3.7-eV^2 2ν solutions are about as high as for the 3ν solution. In particular the 3ν solution incorporates both the $\delta m^2=0.9-\text{eV}^2$ and $\delta m^2=2.3-\text{eV}^2$ oscillations as in the 2ν solutions and with similar magnitudes of oscillation. Because of the closeness of confidence levels of the 2ν and 3ν oscillation solutions we cannot draw a strong conclusion whether the oscillation solutions prefer one or two effective oscillation terms.

The $\bar{\nu}_e$ spectrum obtained with the 3ν solution with the e^- inversion constraint deviates by less than 10% from the spectrum of Ref. 8 and is within the inversion limits. The $\bar{\nu}_e$ spectrum for the 3ν solution without the e^- constraint is higher than the spectrum of Ref. 8 and would fit within the bounds only if there is a 17% shift in relative normalization between the reactor experiments and the e^- spectrum.

In Fig. 7(c) we show the $P(L/E)$ plot of the survival probability, Eq. (12.3), for the 3ν oscillation solution and compare it to the observed data divided by the values expected from the fitted $\bar{\nu}_e$ spectrum without the oscillation term.

We note that the R_e values for the 3ν solution [Eq. (12.1)] are 6.4 and 8.1 for the 8.7- and 11.2-m experiments, respectively, to be compared with their experimental values of 5.9 ± 0.6 and 8.4 ± 0.8. In addition, for that solution the ratio $\Gamma(\text{ccd})/\Gamma(\text{ncd})$ equals 0.29 to be compared to the weighted mean of the experimental measurements at 11.2 m of $\bar{r}_d=0.23\pm0.06$.

XIII. INCLUSION OF THE 6-m EXPERIMENT INTO THE JOINT ANALYSIS

So far we have disregarded the 6.5-m experiment of Nezrick and Reines[3] because the statistics in that experiment were much poorer compared to the 8.7 and 11.2-m IB experiments. In addition, as we had discussed before the reactor-off background determination in that experiment was very poor. The number of events, especially in the high-energy ($E_e\gtrsim4$ MeV) bins, is so few that by using Poisson statistics the information on the detailed shape of the spectrum gets so dilute that it cannot be used for drawing any reliable conclusions. So instead of dividing the data into 0.5-MeV bins we divide it into two bins, i.e., $2.2<E_e<4.4$ MeV with 155 ± 28 events and $4.4<E_e<6.7$ MeV with 88 ± 18 events.

We now include these two data points from the 6.5-m experiment along with the 8.7- and 11.2-m IB and ccd and ncd rates at 11.2-m and search for a joint no-oscillation spectrum of arbitrary shape. We find that the best no-oscillation fit to the above data set has $\chi^2/d_f=49.5/26$ (C.L.$=0.0035$). Of this the high-energy 6.5-m bin contributes $\chi^2{}_{6H}=9.8$ and the low-energy bin $\chi^2{}_{6L}=2.1$. In comparison the joint 3ν oscillation solution also including the two 6.5-m bins above has essentially the same parameters as the 3ν solution without the 6.5-m bins and without the e^- inversion constraint and gives $\chi^2/d_f=31.6/22$ (C.L.$=0.085$). The 6-m bins with this fit would give $\chi^2{}_{6H}=6.7$ and $\chi^2{}_{6L}=0.7$. Comparing no-oscillation to 3ν oscillation solutions there is a gain in confidence level by a factor of 24. While the 3ν oscillation solution is in agreement with the 8.7-m, 11.2-m, and deuteron experiments and low-energy 6.5-m bin it fails on the high-energy 6.5-m bin giving a value of 40 events compared to experiment with 88 ± 18 events. This is again reflected in the R_e values of the 3ν solution $R_e(6)=5.4$, $R_e(8)=6.2$, $R_e(11)=8.2$ and $\Gamma(\text{ccd})/\Gamma(\text{ncd})=0.26$ agreeing with experiment except for 6.5 m; $R_e^{\text{exp}}(6)=3.3\pm0.7$, $R_e^{\text{exp}}(8)=5.9\pm0.6$, $R_e^{\text{exp}}(11)=8.4\pm0.8$, and $\bar{r}_d=0.23\pm0.06$. Thus the enhanced rates seen in the 6.5-m experiment for $E_e\gtrsim4.5$ MeV cannot be satisfactorily accounted for either with or without oscillations.

We next discuss the 2ν oscillation solutions for the same data sets, i.e., with the data from all the four experiments with only the stated two data bins from the 6.5-m experiment. The three solutions that appeared in the data set without the 6.5-m experiment still appear with the parameters

only slightly changed. For the $(\delta m^2, \sin^2 2\theta)$ values the χ^2 are

δm^2	$\sin^2 2\theta$	χ^2/d_f	C.L.	χ^2_{6H}
0.93 eV^2	0.43	40.1/24	0.021	7.7
2.36 eV^2	0.23	37.4/24	0.039	8.4
3.75 eV^2	0.29	37.9/24	0.034	10.6

All of these solutions are in reasonable agreement with the data from the 8.7-m, 11.2-m, and deuteron experiments and none of them can satisfactorily account for the broad enhancement in the rates for $E_e \gtrsim 4.5$ MeV observed by the 6.5-m experiment. Out of the three solutions, the 0.9-eV^2 solution is somewhat better for that experiment than the other two solutions.

XIV. CONSISTENCY WITH BOUNDS FROM ACCELERATOR EXPERIMENTS

Experiments at accelerators have set limits on neutrino flavor transition oscillations and shown them as plots in the δm^2, $\sin^2 2\theta$ plane.

A probability limit $\Delta P_{\text{C.L.}} < 1$ for nondetection at a given confidence level gives a bound on $(\delta m^2)^2 \sin^2 2\theta$ found by expanding the $\sin^2(2.53 \delta m^2 L/2E)$ term in (9.12) for two neutrinos [similarly for the pseudo-2ν case in (9.17)],

$$\sin^2 2\theta \left[\frac{2.53 \delta m^2 L}{2E} \right]^2 \leq \Delta P_{\text{C.L.}} \, . \tag{14.1}$$

Experimental constraints modify this simple parabolic relation at very small $\sin^2 2\theta$.

The recent reanalysis of the neutrino experiment at LASL for oscillation bounds by Nemethy *et al.*[9] and the bubble-chamber experiment of Baltay *et al.*[10] at Fermilab have set the strongest current bounds for low δm^2. These are shown in Fig. 9 along with our 90% contours.

For the simple case of only 2ν mixing none of the bounds is inconsistent with the $\delta m^2 = 0.9$-eV^2 region. The $\delta m^2 = 2.3$ eV^2 and the $\delta m^2 = 3.7$ eV^2 regions are inconsistent with $\nu_e \leftrightarrow \nu_\mu$ but not with $\nu_e \leftrightarrow \nu_\tau$.

XV. IMPLICATIONS FOR NEW REACTOR EXPERIMENTS

Experiments are now in progress to measure the IB reaction each of which uses a moveable detector

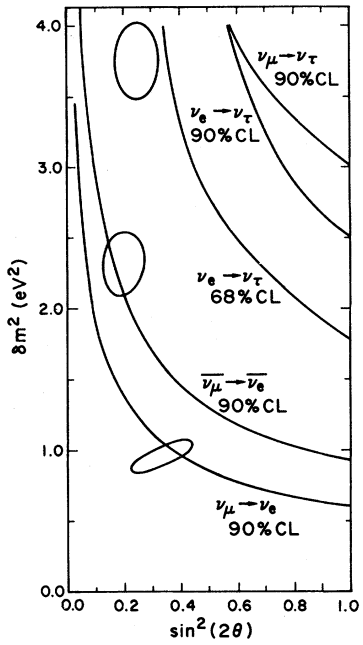

FIG. 9. Our oscillation solutions are compared with limits from accelerator experiments. The limits on $\nu_\mu \to \nu_e$ and $\nu_\mu \to \nu_\tau$ are from Ref. 10 and the remaining limits are from Ref. 9. The $\nu_e \to \nu_\tau$ limits do not exclude any of our solutions. The $\delta m^2 = 0.9$-eV^2 solution is also not excluded by $\nu_\mu \to \nu_e$ or $\bar{\nu}_\mu \to \bar{\nu}_e$. However the $\delta m^2 = 2.3$-eV^2 and $\delta m^2 = 3.7$-eV^2 solutions are excluded from being mainly $\nu_\mu \leftrightarrow \nu_e$ oscillations.

at different distances from the same reactor.[34] In the long-term mode of these experiments one can look for a change in the positron spectrum with distance holding normalization, energy calibration, and resolution stable without needing to make an accurate determination of these. In comparing different experiments, obtaining a good energy resolution and precise energy calibration are essential. Also at a power reactor the time dependence of the reactor composition of $^{235}\text{U} \to {}^{239}\text{Pu}$ will have to be accounted for. The parameters for neutrino oscillation that emerge from our work are characterized by small mixing angles of the order of Cabibbo angles. The oscillation amplitudes are small, of the order of 25%, and emphasize the necessity for stable high-statistics experiments.

In order to determine the most favorable distances to position a detector implied by the joint oscillation solutions we compute the e^+ spectrum that the detector would measure at each distance L with the solutions. We then compare that rate $R(E_i, L)$ with, for example, the spectrum measured at 8.7 m at ILL, $R(E_i, 8.7)$ with errors σ_i, and compute the χ^2 deviation for each L,

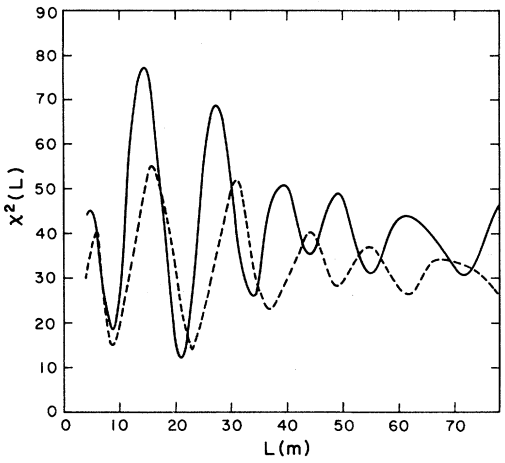

FIG. 10. $\chi^2(L)$ [defined in Eq. (15.1)] for a measurement at L compared to the 8.75-m data for the oscillation solutions with 2ν: $\delta m^2=0.95$ eV^2 (solid line) and 3ν (dashed line). The uncertainty is $\Delta L/L\simeq 10\%$.

$$\chi^2(L)=\sum_{i=1}^{19}\left[\frac{R(E_i,L)-R(E_i,8.7)}{\sigma_i(8.7)}\right]^2, \quad (15.1)$$

assuming that the number of events measured at L is much larger than that at 8.7 m so the fluctuations at L are much smaller than $\sigma_i(8.7)$. We also assume a moveable detector so that there are no relative normalization or energy-calibration differences.

Figure 10 shows a graph of $\chi^2(L)$ vs L for the $\delta m^2=0.95$-eV^2 2ν solution and for the 3ν solution, Eq. (12.2). This calculation is done with the characteristics of the 8.7-m detector at a large reactor (SRP). (The time dependence of the reactor composition $^{235}\mathrm{U}\rightarrow{}^{239}\mathrm{Pu}$ will have to be corrected for in a long-cycle power reactor.) The curves or locations of maximas and minimas have an uncertainty of about $\Delta L/L\simeq 10\%$ due to the allowed range of δm^2. The 2.3 and 3.7-eV^2 2ν solutions are not plotted since they show smaller variations due to reactor size damping. The 3ν solution shows smaller variation since the coefficient of its 0.9-eV^2 component is smaller than in the 2ν 0.9-eV^2 solution and the 2.3-eV^2 component is damped. The disappearance channel for these high-mass solutions can only be determined oscillating at the smaller ILL reactor and we encourage future experiments there. The high δm^2 may also be examined in accelerator appearance experiments (i.e., $\nu_e\leftrightarrow\nu_\mu$) or by monitoring the produced kaon flux at one distance and simultaneously measuring the ν_e flux further downstream.

It seems to us that the measurement of the $\bar{\nu}_e$ spectrum at distances $\lesssim 11.2$ m could be particularly important. We have tried to account for the observed distance dependence in the $\bar{\nu}_e$ spectrum by using the simplest possible theory of flavor oscillations. One can imagine completely different theoretical scenarios whose evolution beyond those three distances may be entirely different from the simple oscillation solutions we have investigated. We take special note of the fact that our oscillation solutions are not able to account for the 6.5-m bins for $E_\nu\geq 6$ MeV to our satisfaction. We attribute this to the poor background determination at high energies. However, it is within the realm of possibilities that the apparent high-energy-bin excess is correct. In that case it is signifying something more subtle than the standard 2ν and 3ν oscillation theory that we have investigated here. A new measurement of the $\bar{\nu}_e$ spectrum at 6.5-m may prove very rewarding.

We have studied the ccd disintegration rate as a function of distance for each of our three solutions. Once again the 0.9-eV^2 solution exhibits clear variations for distances $\lesssim 40$ m. The other two solutions settle down to their asymptotic values very rapidly. While the deuteron-disintegration experiment has the obvious disadvantage of a much smaller cross section than IB it also presents one with some advantages. No precise energy measurements are involved. As noted by RSP[6] the ratio $\Gamma(\mathrm{ccd})/\Gamma(\mathrm{ncd})$ is remarkably insensitive to reactor $\bar{\nu}_e$ spectra. Second-generation experiments dedicated towards an improved measurement of the ccd and ncd rates as a function of distance can provide important information on ν instability. While in the standard model of electroweak interactions the ncd rate is expected to be independent of distance[22] one can have $\bar{\nu}_e$'s oscillate to some ν or $\bar{\nu}$ that does not couple to nucleons via the weak neutral current at least as dictated by the Weinberg-Salam theory. A measurement of the ncd reaction as a function of distance would therefore provide a useful probe for the underlying gauge interactions.

XVI. CONCLUSIONS AND SUMMARY

We have presented a phenomenological analysis of the data from four experiments initiated by reactor $\bar{\nu}_e$ and done at 6.5,[3] 8.7,[4] and 11.2 m.[5] Three of these were IB experiments performed at these distances and one of them was the deuteron-disintegration experiment also performed at 11.2 m. We recall that Reines, Sobel, and Pasierb[6] used

the results of their deuteron experiment only and presented the observed value of the ratio ccd/ncd and its expected value based on theoretically calculated spectra as evidence for neutrino instability.

We find that the $\bar{\nu}_e$ spectra measured in the three IB experiments show a statistically significant distance dependence. In particular, at 11.2 m, both the IB experiment on protons and the deuteron experiment monitor $\bar{\nu}_e$ spectra that are considerably softer (for $E_\nu \gtrsim 6$ MeV) than the ones observed at 8.7 and 6.5 m. With increase in distance the data exhibit a systematic depletion of higher energy ($E_\nu \gtrsim 6$ MeV) $\bar{\nu}_e$'s relative to lower-energy ones. The values of the ratios R_ν extracted from the three IB experiments are different (taken in pairs) by ≥ 2.9 standard deviations, and the shape differences cannot be accounted for by normalization or energy-calibration shifts.

We have searched for joint no-oscillation fits to the spectra monitored at different distances. In so doing we have allowed the joint spectrum to have any arbitrary shape. We assume only that the spectrum is a smooth function of neutrino energy. Justification for this assumption is given in Sec. III. We allow for variations in the absolute normalization and in e^+ energy calibration of individual experiments. The spectra monitored at each distance are remarkably different in shape (see Sec. V). The confidence level for the joint no-oscillation fit to even the partial set of overlapping data from the 8.7 and 11.2-m IB experiments alone, is C.L.$=0.026$. Even with substantial relaxation in the energy-calibration uncertainties the confidence level was found to be <0.10.

Assuming a simple two-component form for neutrino oscillations we find a set of three solutions to all the reactor data. These have the values $\delta m^2 = 0.95 \pm 0.10$ eV^2, 2.34 ± 0.23 eV^2, 3.75 ± 0.27 eV^2 with $\sin^2 2\theta = 0.32 \pm 0.11$, 0.20 ± 0.07, 0.25 ± 0.08, respectively. The three-neutrino solution to the same data contains a linear combination of the 0.9- and 2.4-eV^2 solutions with coefficients of 0.17 and 0.16, respectively, replacing $\sin^2 2\theta$ in the 2ν case. With the introduction of only two oscillation parameters in the 2ν case the χ^2, on the same subsets as the no-oscillation tests are made, show reductions by as much as 8 to 11 units. The confidence levels on the fits with the oscillation solutions are about an order-of-magnitude larger than without oscillations. The oscillation solutions exist with high confidence level even when the reactor $\bar{\nu}_e$ spectra is constrained to be within the range of the $\bar{\nu}_e$ spectrum obtained by inversion[7,8] of the measured β spectrum from fission of ^{235}U.

The inclusion of the 6.5-m data with their large statistical errors does not significantly alter the solutions. The solutions do not account for the excess of events seen at the high-energy end at 6.5 m. Because of this the best 3ν oscillation solution including the 6.5-m data has C.L.$=0.09$ which is, however, still much larger than the no-oscillation solution with C.L.$=0.004$.

The oscillation solutions resulting from our joint analysis depend mostly on the interplay of the shape differences between 8.7- and 11.2-m IB (Fig. 1) and the overall spectral constraint of ncd. The 90%-C.L. contours of the oscillation solutions (Fig. 6) lie within the 68% contours of Boehm *et al.*[4] (Fig. 8) which they obtain by using only their 8.7-m data and the spectrum of Ref. 8. This overlap using an independent set of experiments from Boehm *et al.* is nontrivial and indicates the compatibility of all of the experiments.

The amplitude for oscillation resulting from our joint analysis of all the reactor data is somewhat smaller than that resulting from the RSP analysis of only their deuteron experiment. Most of this difference arises because of the 1.07-SD difference in the ccd rate as measured by the deuteron experiment and used by RSP and that implied by the 11.2-m IB experiment (including now calibration errors), i.e., the spectrum measured by the latter experiment is somewhat higher at the higher-energy end than that implied by the deuteron experiment. New contours for the deuteron experiment with the best-fit spectrum for the $\delta m^2 = 0.9$ eV^2 solution and the weighted mean of the ratio $\bar{r} = \langle \Gamma(\text{ccd})/\Gamma\ (\text{ncd}) \rangle = 0.23 \pm 0.06$ are shown in Fig. 11. Due to the large errors on Γ(ccd) it did not carry much weight in the joint experimental analysis. Thus it is important for consistency of the experiments that our contour at $\delta m^2 \simeq 0.95$ eV^2 lies within the 90%-C.L. contours of the RSP analysis which was based only on the ccd and ncd data and the calculated spectrum of Ref. 15.

Our oscillation solutions are not ruled out by accelerator experiments.[9–13] These experiments are not sufficiently sensitive to small-amplitude oscillations (with angles $\sim$ Cabibbo angles) in the range of $\delta m^2 \sim 1$ eV^2 which emerge favorably from our analysis.

If neutrino oscillations are not introduced to account for the distance dependence that we exhibit then at least three of the four reactor experiments must have unstated sources of error or seriously understated errors. Specifically, it is not enough to account for the observed differences in the IB measurements at 8.7 and at 11.2 m by attributing them

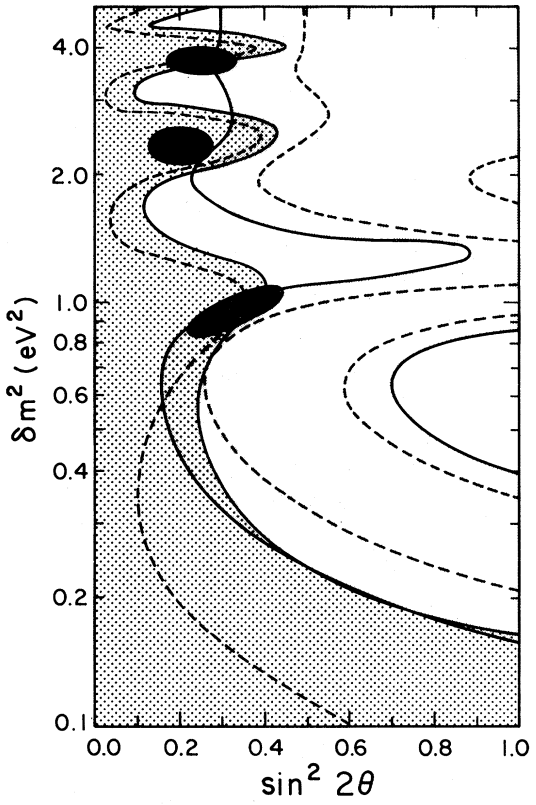

FIG. 11. The allowed region to the left of the contours on the left results from the analysis by Boehm *et al.* of their own IB experiment at 8.7 m. The allowed region to the right of the contours on the right-hand side results from our analysis of the ratio $r=\bar{\Gamma}(\text{ccd})/\Gamma(\text{ncd})$ from the weighted mean of the ccd rate measured directly in the deuteron experiment and that implied by the IB experiment at 11.2 m (see Sec. VI) and the best-fit reactor $\bar{\nu}_e$ spectra for the $\delta m^2=0.9$-eV^2 solution. The 90%-C.L. contours for the allowed region resulting from our joint analysis of all reactor experiments are shown darkly shaded.

to, e.g., an $\sim 7\%$ relative calibration shift in e^+ energy between the two experiments. Firstly a joint no-oscillation fit to these two experiments is still improbable (C.L. <0.10). In addition the deuteron measurement of $\Gamma(\text{ccd})/\Gamma(\text{ncd})$ would also have to be in error by $\gtrsim 2$ SD.

In contrast, simple two-component oscillations are able to account for the data reasonably well and the resulting oscillation solutions are not incompatible with any other relevant information currently available, e.g., reactor $\bar{\nu}_e$ spectrum obtained by inversion of the measured β spectrum, or constraints from accelerator experiments.

We are therefore led to suggest that neutrino oscillations rather than experimental inaccuracies are the more likely cause of the distance dependence that we have presented.

Note added in proof. Since this paper was submitted for publication two reactor experiments have been completed. First, the Caltech-SIN-München Collaboration [J. L. Vuilleumier *et al.*, SIN Report No. PR-82-07 (unpublished)] have reported a measurement of the e^+ spectrum at 38 m from a power reactor at Gösgen. Using the reactor $\bar{\nu}_e$ spectrum obtained from inversion of the measured e^- spectrum from ^{235}U and from ^{239}Pu, and without including the Z-dependent inversion uncertainties in their analysis, they report that they do not find any evidence for neutrino oscillations. Second is the experiment of A. A. Borovoi *et al.* [see Oak Ridge National Laboratory English translation of the Russian Report No. ORNL-tr-4842, 1982 (unpublished)], which measures the e^- spectrum from ^{235}U and ^{239}Pu and finds it appreciably higher than that used in the analysis of Vuilleumier *et al.* These two experimental results do not appear to be compatible and they, once again, underscore (as is stressed in our analysis) the problems with the e^- inversion method. The question of small-amplitude oscillations (of the type relevant to this work) can be convincingly settled only by measuring the $\bar{\nu}_e$ spectrum at several distances from a reactor.

ACKNOWLEDGMENTS

We wish to thank F. Reines, H. Sobel, and E. Pasierb for generous cooperation in aiding our understanding of the experiments with many helpful discussions and reviews. We also wish to thank for discussions J. J. Sakurai, H. Chen, F. Nezrick, P. Vogel, F. Avignone, A. Hahn, F. Boehm, G. Shaw, J. Dorfan, and B. P. Roe. This work was supported in part by the National Science Foundation under Grants Nos. PHY-78-21502 and PHY-79-10262.

APPENDIX: REACTOR-SIZE EFFECT

In this appendix we treat the effects of reactor-core size in damping the oscillating terms. First we make some general observations and then treat a uniform spherical source approximation which is used in the fitting calculations.

For the Savannah River Plant (SPR) the reactor core has a radius of about $R=2.3$ m and its size must be considered for values of δm^2 and E where the size is a fraction of the oscillation length

$\lambda=(2\pi/2.53)E/\delta m^2$. The detector size is 0.2 m and can be neglected here. For $R\sim\lambda/4$ at $E=4$ MeV it will be important for $\delta m^2\gtrsim 1$ eV^2. For oscillation lengths λ of the order or smaller than the reactor size the oscillations will be averaged out. For $R\simeq\lambda$ at $E=4$ MeV this sets a limit of $\delta m^2\lesssim 4$ eV^2 beyond which the oscillation term will be severely damped.

The neutrino source will be treated as geometrically small compared to the distance L_0 from the detector to the center of the source ($R\ll L_0$) so that we can use only the longitudinal distance L_0-z from a point in the source z to the detector $\{L=[(L_0-z)^2+x^2+y^2]^{1/2}\simeq L_0-z\}$. The source strength at distance z from the center is then $S(z)=\int dx\,dy\,S(x,y,z)$.

The oscillating term $\cos(bL)$ is then averaged over the source size $|z|\le R$ using $L=L_0-z$:

$$\langle \cos bL\rangle_S=\frac{\int_{-R}^{R} dz\cos[b(L_0-z)]S(z)}{\int_{-R}^{R} dz\,S(z)}\ . \tag{A1}$$

Expanding $\cos(bL_0-bz)$ and using the fact that $S(z)$ is even in z we get

$$\langle \cos bL\rangle_S=\cos(bL_0)D(bR)\ , \tag{A2}$$

where

$$D(b,R)=\frac{\int_{-R}^{R} dz\cos(bz)S(z)}{\int_{-R}^{R} dz\,S(z)}\ . \tag{A3}$$

So the integration over the source still gives a simple oscillation with distance L_0 from the source center but damped by $D(b,R)$ which is independent of L_0 and has $|D(b,R)|\le 1$.

For a uniform spherical source of radius R with $S(x,y,z)=\rho$ then $S(z)=\pi\rho(R^2-z^2)$, and

$$D(bR)=3[\sin(bR)-bR\cos(bR)]/(bR)^3\ , \tag{A4}$$

where $b=2.53\delta m^2(\text{eV}^2)/E(\text{MeV})$. The actual neutrino source at SRP is geometrically more complicated than a uniform sphere but can be well approximated by one for $\delta m^2<3$ eV^2. The equivalent radius $R=2.16$ m is chosen to give the same ratio of uniform central output to total output as for the actual nearly spherical reactor source.

For $\delta m^2=1$ eV^2 the damping at $E=4$ MeV is only $D(bR)=0.83$ but at $\delta m^2=3$ eV^2 and $E=4$ MeV the damping factor is $D(bR)=0.07$. At $E=6$ MeV the damping is less and for $\delta m^2=1$ eV^2, $D(bR)=0.92$ and for $\delta m^2=3$ eV^2, $D(bR)=0.43$.

For a rectangular detector of half-width R the damping function is $D(bR)=\sin(bR)/bR$. Taking both reactor and detector sizes into account results in another integral over L_0 in (A2) for the detector size and gives a damping function that is the product of the reactor and detector damping functions.

[1]A brief summary of this analysis has been published. See D. Silverman and A. Soni, Phys. Rev. Lett. 46, 467 (1981).

[2]See also D. Silverman and A. Soni, in *Gauge Theories, Massive Neutrinos, and Proton Decay,* proceedings of Orbis Scientiae, Coral Gables, 1981, edited by A. Perlmutter (Plenum, New York, 1981), p. 249.

[3]F. Nezrick and F. Reines, Phys. Rev. 142, 852 (1966).

[4]Caltech-ILL-ISN-Munich Collaboration, F. Boehm *et al.*, Phys. Lett. 97B, 310 (1980); H. Kwon *et al.*, Phys. Rev. D 24, 1097 (1981).

[5]F. Reines, H. S. Gurr, and H. W. Sobel, reported by H. W. Sobel, in *Neutrino Physics and Astrophysics,* proceedings of the International Conference, Erice, Italy, 1980, edited by E. Fiorini (Plenum, New York, 1982).

[6]F. Reines, H. W. Sobel, and E. Pasierb, Phys. Rev. Lett. 45, 1307 (1980).

[7]R. E. Carter, F. Reines, J. J. Wagner, and M. E. Wyman, Phys. Rev. 113, 280 (1959).

[8]K. Schreckenbach *et al.*, Phys. Lett. 99B, 251 (1981).

[9]P. Nemethy *et al.*, Phys. Rev. D 23, 262 (1981).

[10]BNL-Columbia experiment, C. Baltay *et al.*, in Proceedings of the Neutrino Oscillation Workshop, Brookhaven National Laboratory, 1981 (unpublished).

[11]Bari-Birmingham-Brussels-Ecole Polytechnique-Rutherford-Saclay-UCL Collaboration, O. Erriquez *et al.*, CERN report, 1981 (unpublished).

[12]For a recent review, see Lawrence W. Jones, University of Michigan Report No. UMH-E.81-23, presented at the XVI Rencontre de Moriond, Les Arcs, Savoie, France, 1981 (unpublished).

[13]B. P. Roe, talk presented at the Neutrino Oscillation Workshop, Brookhaven National Laboratory, 1981 (unpublished).

[14]F. T. Avignone and Z. D. Greenwood, Phys. Rev. C 22, 594 (1980).

[15]B. R. Davis, P. Vogel, F. M. Mann, and R. E. Schenter, Phys. Rev. C 19, 2259 (1979).

[16]P. Vogel, G. K. Schenter, F. M. Mann, and R. E. Schenter, Phys. Rev. C 24, 1543 (1981).

[17]A. A. Borovoi, Yu. L. Dobryuin, and V. I. Kopeikin,

Yad. Fiz. 25, 264 (1977).
[18]S. A. Fayan, L. A. Milaelyas, and Y. L. Dobryuin, J. Phys. 5G, 209 (1979).
[19]V. I. Kopeikin, Yad. Fiz. 32, 62 (1980).
[20]B. Gabioud *et al.*, Phys. Rev. Lett. 42, 1508 (1979); W. R. Gibbs and G. J. Stephenson, Jr., Phys. Rev. D 23, 260 (1981). See also F. T. Avignone, *ibid.* 24, 778 (1981); T. Ahrens and L. Gallaher, *ibid.* 20, 2714 (1979).
[21]W. R. Gibbs *et al.*, Phys. Rev. C 11, 90 (1975); 12, 2130 (1975).
[22]This is true only for mixing among ν_{eL}, $\nu_{\mu L}$, $\nu_{\tau L}$ doublets. See, e.g., V. Barger, P. Langacker, J. P. Leveille, and S. Pakvasa, Phys. Rev. Lett. 45, 692 (1980).
[23]In addition to Refs. 7 and 8 there are other reported measurements of the β spectrum from fission of ^{235}U. See N. Tsoulfanides, B. W. Wehring, and M. E. Wyman, Nucl. Sci. Eng. 43, 42 (1971).
[24]See also J. K. Dickens *et al.*, Nucl. Sci. Eng. 74, 106 (1980).
[25]B. Pontecorvo, Zh. Eksp. Teor. Fiz. 33, 549 (1957); 34, 247 (1958); 53, 1717 (1967) [Sov. Phys.—JETP 6, 429 (1958); 7, 172 (1958); 26, 948 (1968)]; Z. Maki *et al.*, Prog. Theor. Phys. 28, 870 (1962); Y. Katayama *et al.*, *ibid.* 28, 675 (1962); M. Nakagawa *et al.*, *ibid.* 30, 727 (1963); V. Gribov and B. Pontecorvo, Phys. Lett. 28B, 493 (1969).
[26]S. M. Bilenky and B. Pontecorvo, Phys. Rep. 41C, 225 (1978); L. Wolfenstein, Phys. Rev. D 20, 2634 (1979); A. K. Mann and H. Primakoff, *ibid.* 15, 655 (1977).
[27]A. De Rújula, L. Maiani, S. Petcov, and R. Pentrozio, Nucl. Phys. B168, 54 (1980); S. M. Bilenky, J. Hosek, and S. T. Petcov, Phys. Lett. 94B, 495 (1980).
[28]V. Barger, D. Cline, K. Whisnant, and R. J. N. Phillips, Phys. Lett. 93B, 194 (1980). This paper was the first to use the neutrino spectra from the 6- and 11-m IB experiments for neutrino oscillations. As we have stressed in the text the 6-m experiment had low statistics and poor background determination. The small event rate in each individual bin requires the use of Poisson statistics whereby the detailed shape of spectrum does not get constrained enough to enable one to draw any reliable conclusions. See Sec. XIII.
[29]S. Pakvasa, in *Proceedings of the 1980 DUMAND Symposium, Honolulu,* edited by V. J. Stenger (Hawaii DUMAND Center, Honolulu, 1981), Vol. 2, p. 45.
[30]V. A. Lubimov, E. G. Novikov, V. Z. Nozik, E. F. Tretyakov, and V. S. Kosik, Phys. Lett. 94B, 266 (1980).
[31]B. Kayser, Phys. Rev. D 24, 110 (1981).
[32]N. Cabbibo, Phys. Lett. 72B, 333 (1978); L. Wolfenstein, Phys. Rev. D 18, 958 (1978); V. Barger, K. Whisnant, and R. J. N. Phillips, Phys. Rev. Lett. 45, 2084 (1980).
[33]This was also done independently by S. Pakvasa (private communication).
[34]Oscillation experiments to measure reaction (1.1) as a function of distance are underway by Reines *et al.* and by Boehm *et al.*